DOI: 10.1070/RCR4811

Nanosized vehicles for delivery of photosensitizers in photodynamic diagnosis and therapy of cancer

Andrey F.Mironov, Kseniya A.Zhdanova, Natal'ya A.Bragina

MIREA — Russian Technological University
prosp. Vernadskogo 86, 119571 Moscow, Russian Federation

The review summarizes the state of the art of research in the field of nanosized vehicles for delivery of photosensitizers for diagnosis and treatment of malignant neoplasms by photodynamic cancer therapy. Data on the utilization of porphyrin- and phthalocyanine-based photosensitizers in medical practice, the employment of vehicles for their delivery and the development of new effective medications are considered. The review focuses on the most commonly used and proven vehicles based on lipids, lipoproteins and polymers. Strategies for increasing efficiency of nanosized delivery vehicles using various vector molecules specific to different types of cancer are discussed. A systematic analysis of the published data is presented and the available tools for increasing the efficacy of photodynamic therapy by means of nanosized delivery vehicles are assessed.
The bibliography includes 188 references.

Contents

1. Introduction 859
2. Basics of photodynamic therapy 860
3. Photosensitizers for photodynamic therapy of cancer 861
4. Main delivery vehicles for photosensitizers 863
5. Conclusion 878

1. Introduction

Along with cardiovascular diseases, cancers are among the leading causes of human deaths worldwide. Despite significant advances in this area, malignant neoplasms remain a great challenge for modern medicine. Thus, a half million of new cases of cancer are newly diagnosed each year in Russia. Traditional cancer treatment methods, such as surgery, radiation therapy and chemotherapy, have serious drawbacks. Therefore, the development of new treatment methods available and acceptable to patients is an extremely important area of modern research in medicine.

A relatively new cancer treatment called photodynamic therapy (PDT) offers a promising approach to diagnosis and treatment of malignant neoplasms.[1 – 3] Photodynamic therapy is a binary treatment that involves the administration of a nontoxic photosensitizer (PS) to cancer cells followed by exposure to laser light, thereby generating reactive oxygen species (ROS), which damage vital cellular components, leading to cell death. This method allows the diagnosis of tumours in early stages, the determination of tumour margins during the PDT treatment procedure and the tumour ablation, while preserving healthy tissues. Compared to the other methods currently used in oncology, PDT has the advantages of minimal invasiveness and extremely low systemic toxicity.[4, 5]

In 2012, the Ministry of Health of the Russian Federation included this method in the official list of standards of care for patients with cancer. Photodynamic therapy proved to be efficient in the treatment of some types of cancer, such as skin, lung, bladder cancers, brain tumour, head and neck cancer and esophagus cancer. This method is also used as an adjuvant therapy to surgery to reduce residual tumour burden.

Despite great interest in PDT and its applications, this method is not yet commonly used in clinical practice

A.F.Mironov. Doctor of Chemical Sciences, Professor at the Department of Chemistry and Technology of Biologically Active Compounds, Medicinal and Organic Chemistry of the Lomonosov Moscow State University of Fine Chemical Technology 'MIREA — Russian Technological University'.
E-mail: mironov@mitht.ru
Current research interests: fine organic synthesis, nitrogen-containing heterocycles, pyrrole chemistry, porphyrins, chlorins, bacteriochlorins, photodynamic therapy.
K.A.Zhdanova. PhD (Chemistry), Assistant Lecturer at the same Department.
E-mail: mishkina_ksyusha@mail.ru
Current research interests: synthesis of heterocyclic compounds, *meso*-aryl-substituted porphyrins, nanomedicine.
N.A.Bragina. PhD (Chemistry), Assistant Professor at the same Department.
E-mail: n.bragina@mail.ru
Current research interests: chemistry of macrocyclic compounds, amphiphilic porphyrins, nanomedicine.

Received 7 February 2018
Translation: T.N.Safonova

© 2018 Uspekhi Khimii, Russian Academy of Sciences and Turpion Ltd.

because of a number of limitations, most significant of which are the lack of highly efficient PSs and adequate tumour-targeted PS delivery systems. Studies on the use of nanomaterials for the targeted PS delivery started much later than the development of first PSs. Meanwhile, the application of nanotechnology in PDT has attracted great attention in recent years. Nanoparticles not only provide good solubility of PSs in certain media (hydrophilic, hydrophobic) and serve as delivery vehicles but also address some other issues. In particular, nanoparticles prevent aggregation of hydrophobic PSs in water, which drastically reduces singlet oxygen generation. However, it is hydrophobic PSs that most easily penetrate into cancer cells through the hydrophobic cell membrane and are then accumulated in vitally important cellular compartments, as opposed to hydrophilic compounds, which are distributed in the cytoplasm, thus diminishing the photodynamic effect. Nanoparticles improve PS delivery, primarily the delivery of hydrophobic PSs, to the tumour site both due to migration predominantly through enlarged capillary pores of the tumour tissue and owing to the possibility of attaching targeting ligands to the surface (targeted delivery).

A large body of data has accumulated on the application of different nanoparticles for PS delivery.[6–10] For instance, nanocarriers based on magnetic nanoparticles,[7,8] as well as gold,[6] silicon,[9] carbon (fullerene, graphene) [10] nanoparticles and so on were proposed for this purpose. In recent years, attention has been paid to new IR-absorptive nanoplatforms based on upconversion nanophosphors, which improve PDT efficacy for treating deep-seated tumours in hypoxic environments.[11–13] The use of genetically encoded photosensitizers bearing address domains is another promising PDT-based therapy.[14,15] This approach allows for the selective accumulation of PSs in the tumour loci and makes it possible to control the PS concentration.

This review summarizes the results of studies of liposomal and polymeric biodegradable nanocarriers for photosensitizer delivery, which are most commonly used in fluorescence diagnosis and photodynamic therapy of cancer, approaches to enhancing the efficacy of these nanoparticles and recent advances in clinical cancer treatment.

The following designations and abbreviations are used in the review:

ALA — 5-aminolevulinic acid,
Bchl-BOA — bacteriochlorin e_6 bisoleate,
CD44 — integral cell-surface glycoprotein CD44 (cluster of differentiation 44),
Chl-e_6 — chlorin e_6,
DMPC — dimyristoyl phosphatidylcholine,
DPPC — dipalmitoylphosphatidylcholine,
DPPG — dipalmitoyl phosphatidylglycerol,
DS — drug substance,
EGFR — epidermal growth factor receptor,
ER — endoplasmic reticulum,
HA — hyaluronic acid,
HDL — high-density lipoproteins,
HPPH — 2-(1-hexyloxyethyl)-2-devinyl pyropheophorbide,
ICG — indocyanine green,
LDL — low-density lipoproteins,
mAb — monoclonal antibodies,
MRI — magnetic resonance imaging,
mTHPC — 5,10,15,20-tetrakis(3-hydroxyphenyl)chlorin (temoporfin),
NBD-C6 — 6-{[*N*-(7-nitrobenz-2-oxa-1,3-diazol-4-yl)-amino]hexanoyl}sphingosine,
NP — nanoparticle,
PAMAM — poly(amidoamine),
PC — phosphatidylcholine,
PCL — polycaprolactam,
PDT — photodynamic therapy,
PE — phosphatidylethanolamine,
PEBT — poly[(9,9-dioctylfluorene-2,7-diyl)-*alt*-*co*-(1,4-benzo-2,1,3-thiadiazole)],
PEG — polyethylene glycol,
PET — positron emission tomography,
PGA — polyglycolide,
PLA — polylactide,
PLA-PNIPAM — poly(L-lactide)-block-poly(*N*-isopropylacrylamide),
PLGA — poly(L,D-lactic-co-glycolic) acid,
PNP — polymeric nanoparticle,
PPO — polypropylene oxide,
Proto IX — protoporphyrin IX,
PS — photosensitizer,
pTHPP — 5,10,15,20-tetrakis(4-hydroxyphenyl)porphyrin,
PTT — photothermal therapy,
RES — reticuloendothelial system (mononuclear phagocyte system),
ROS — reactive oxygen species,
SEM — scanning electron microscopy,
SLNP — solid lipid nanoparticles,
TPP — 5,10,15,20-tetraphenylporphyrin,
$TPPS_4$ — 5,10,15,20-tetrakis(4-sulfophenyl)porphyrin,
VEGF — vascular endothelial growth factor.

2. Basics of photodynamic therapy

As mentioned above, PDT is a treatment modality based on a combination of chemotherapy (PS) and the physical stimulus (laser irradiation). After the intravenous administration, PS circulates for some time in the body and is gradually accumulated in the tumour. Then the tumour loci are irradiated with light of appropriate wavelength to activate the PS. This irradiation can be employed for both fluorescence imaging and the formation of cytotoxic reactive oxygen species, *e.g.*, singlet oxygen ($^1O_2$), which oxidizes key cellular macromolecules, resulting in cell death.

The photodynamic effect is generated in the cell by two mechanisms.[16,17] Following light absorption, PS is transformed from the ground state into the short-lived singlet state (^{1}PS), which can be transformed into the relatively long-lived triplet state (^{3}PS) *via* intersystem crossing. In type I reactions, excited triplet-state PS directly reacts with the substrate (*e.g.*, the cell membrane) to form an anion and radical cations, which react with oxygen giving hydroxyl radicals and hydrogen peroxide. In type II reactions, the excited molecule directly reacts with oxygen to form singlet oxygen. The relative contribution of these two types of reactions depends on a number of factors, including the molecular oxygen concentration, the PS structure and the nature of the substrate, but the pathways giving $^1O_2$ generally prevails (Fig. 1).

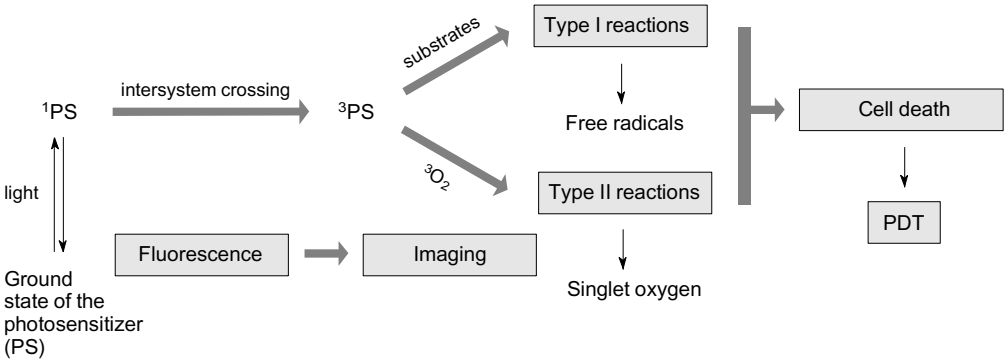


Figure 1. Schematic depiction of physicochemical events underlying photodynamic therapy (PDT).

3. Photosensitizers for photodynamic therapy of cancer

The relationships between the structure of PSs, their transport and accumulation in the cell have been extensively studied. Hydrophobic PSs are characterized by intravenous accumulation due to their transport in the bloodstream by low-density lipoproteins (LDL) followed by endocytosis into cancer cells, wherein LDL receptors are overexpressed.[18] The expression of these receptors in fast-growing cells is associated with high requirements for cholesterol for cell membrane synthesis.[19] Unlike hydrophobic PSs, hydrophilic PSs are carried by serum albumin and are localized in the vascular stroma and intracellular space. The hydrophilic character of these PSs limits their diffusion across the membrane but PSs can be localized in lysosomes *via* endocytosis.[20]

According to some authors, optimal PS should have an amphiphilic character with a certain degree of hydrophobicity sufficient for solubility in water and, at the same time, be hydrophobic to penetrate the outer layer of the cell.[21] The character of cell death greatly depends on the subsequent localization of PS within the cell.

The destruction of cancer cells induced by irradiation can occur *via* necrosis, apoptosis and the autophagy pathway, which has been discovered rather recently. A high PS concentration and high light fluence cause cell necrosis characterized by fast degradation of cellular compartments and plasma membrane destruction followed by the leakage of plasma fluid into the interstitial space.[22] It is generally assumed that necrosis is accidental cell death, although, according to the latest data,[23, 24] programmed cell death is also possible under certain conditions.

Apoptosis is characterized by a decrease in the cell size and the appearance of membrane bubbles in the plasma, but the cell remains intact up to the last stage of programmed death.[25] Since most PSs are not accumulated in the cell nucleus, they do not cause cell mutations. There are correlations between the type of cell death (apoptosis or necrosis) and PS localization in the cells. Thus, the PS localization mainly in the endoplasmic reticulum (ER) or mitochondria leads to apoptosis, while the PS localization in the membrane or lysosomes causes necrosis.[26]

Autophagy is a process wherein cells use their lysosomes or those of neighbouring cells to degrade their own components or whole cells. Unlike necrosis and apoptosis, autophagy is a protective mechanism utilized by eukaryotic cells to eliminate oxidative stress induced by PDT and to prevent structural damage. Consequently, autophagy plays an essential role in cell survival. Depending on the PS structure, the type of cells and experimental conditions, this mechanism can either enhance or suppress the photodynamic effect, thereby stimulating resistance to PDT (Fig. 2).[27 – 29]

Taking into account the key role of the nature of PS on the efficacy of PDT for cancer, the following main requirements for the ideal photosensitizer can be formulated. The ideal PS should have

— high tumour tropicity and low accumulation in normal tissues;

— low cytotoxicity;

— good solubility in water;

— strong absorption in the near-IR region in the so-called 'tissue transparency window' for therapy of large and deep-seated tumours;

— good luminescence for diagnosis;

— high triplet state quantum yield with an energy not lower than 94 kJ mol^{-1} to generate a sufficient amount of ROS.

The design of such PS is a challenging task, if not impossible. Therefore, the development of efficient PSs having an optimal set of spectral and other physicochemical properties, as well as the preparation of adequate nanocarriers for their delivery are important issues for the successful development of PDT of cancer.

Following the historical development and according to the spectral characteristics, photosensitizes can be divided into three generations.[30 – 33] First-generation PS were developed in the 1980 – 1990s based on natural hematoporphyrin IX. These PSs exist as mixtures of monomeric and dimeric porphyrins and high-molecular-weight oligomers.[13] The most well-known PSs of this type are Photofrins I and II (U.S. and Canada), Photosan (Germany) and Photogem (Russia).[34, 35] These PSs effectively destroy tumour blood vessels, have cytotoxicity and are easily soluble in physiological media, which facilitates their intravenous administration; however, these PSs have a number of drawbacks. First, they are highly phototoxic due to accumulation in the skin and slow clearance from the body. Second, they exhibit an absorption band in the therapeutic window at 620 nm, which significantly limits the light penetration depth, and this band has low intensity. The most commonly used

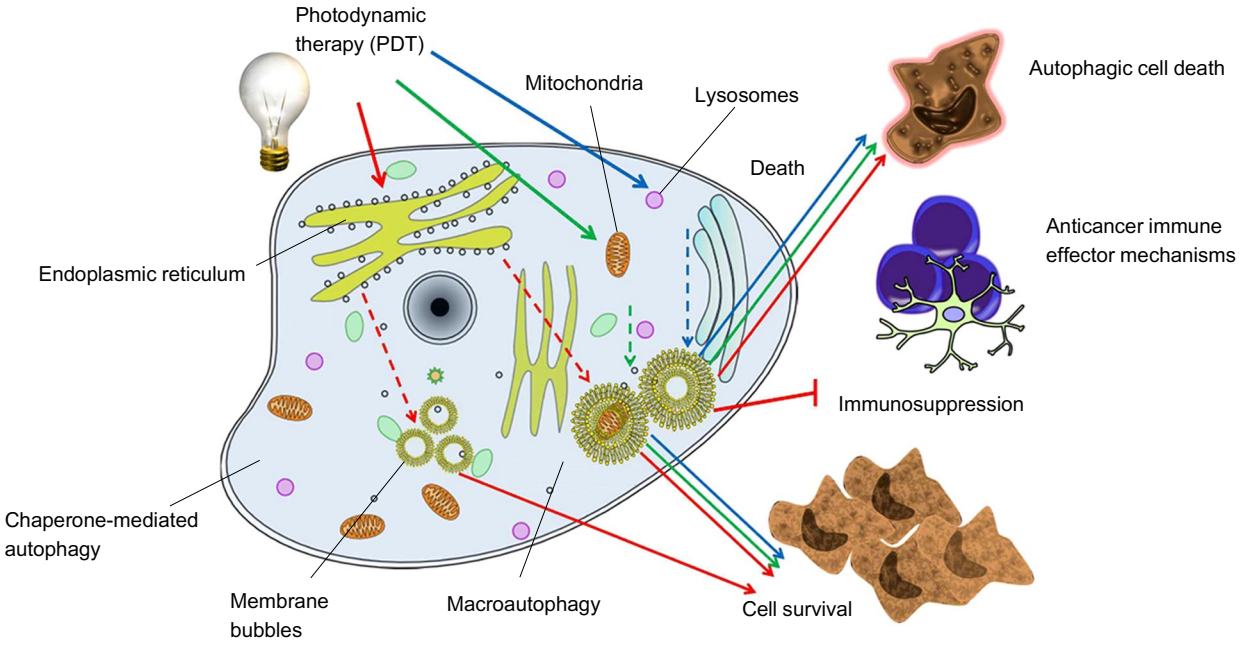
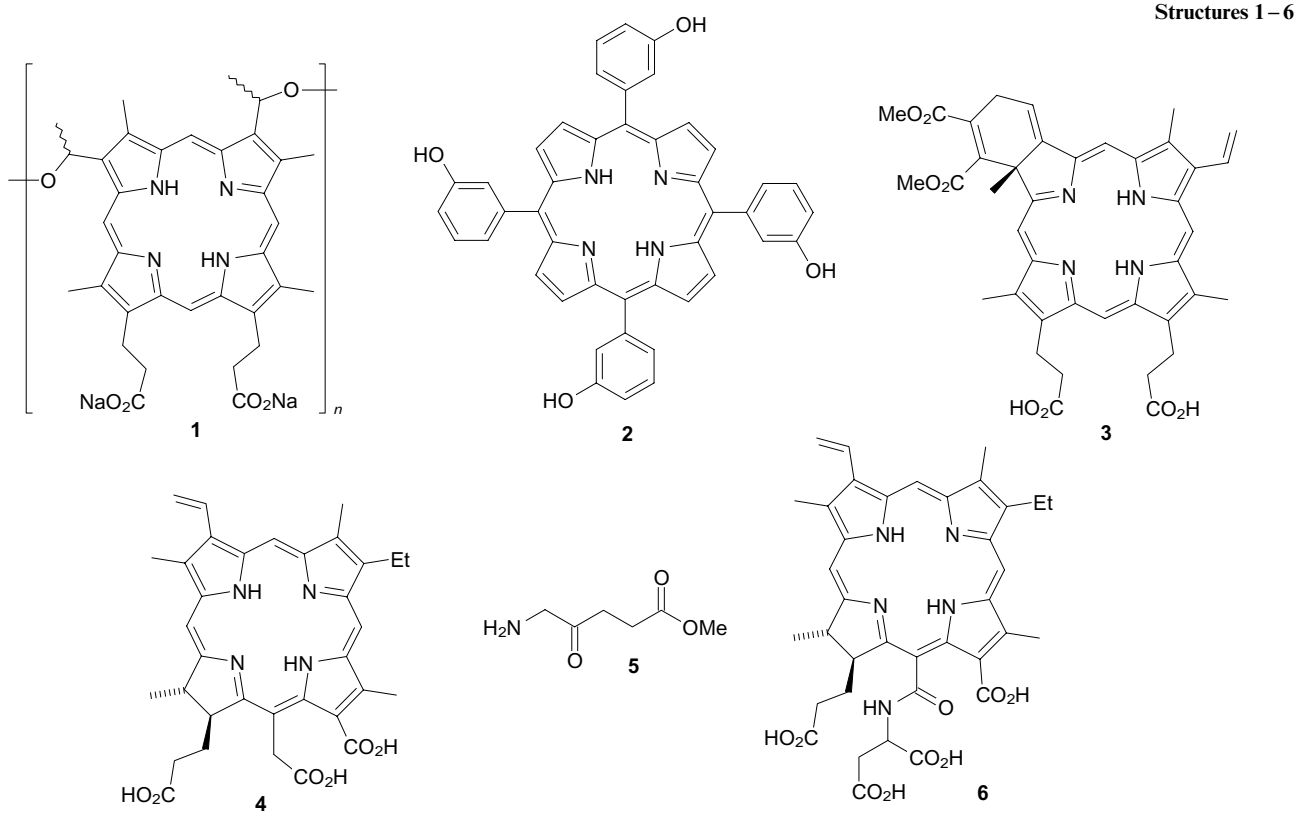


Figure 2. Mechanisms of cell destruction (adapted from Ref. 28). Solid arrows indicate different cell organelles, where PS can be accumulated; dashed arrows indicate the mechanisms of action of PS.

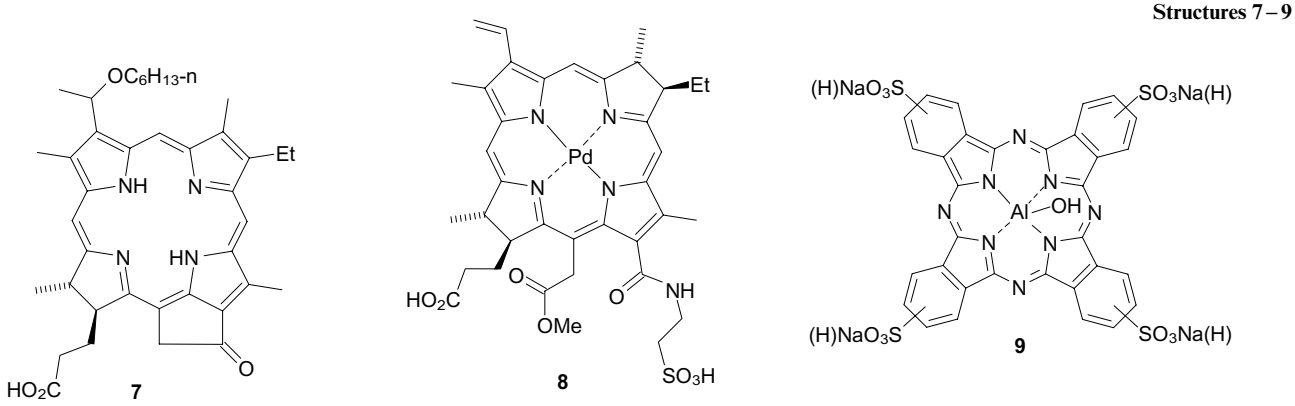
photosensitizers are Hematoporphyrin (Photofrin is its oligomer, **1**), Temoporfin (Foscan, **2**), Verteporfin (Visudyne, **3**), Chlorin e_6 (**4**), 5-aminolevulinic acid methyl ester (Metvix, **5**), Talaporfin (**6**), 2-(1-hexyloxyethyl)-2-devinyl pyropheophorbide *a* (HPPH, **7**), Tookad (**8**) and Photosens (**9**).

However, recent publications can substantially change attitudes to these PSs. A Chinese research group [36] showed that dimeric porphyrin, in which two macrocycles are linked by an oxygen bridge involving vinyl groups of adjacent pyrrole rings, is the most active component of Photofrin II. This PS, which was patented under the name Sinoporphyrin

Structures 1 – 6

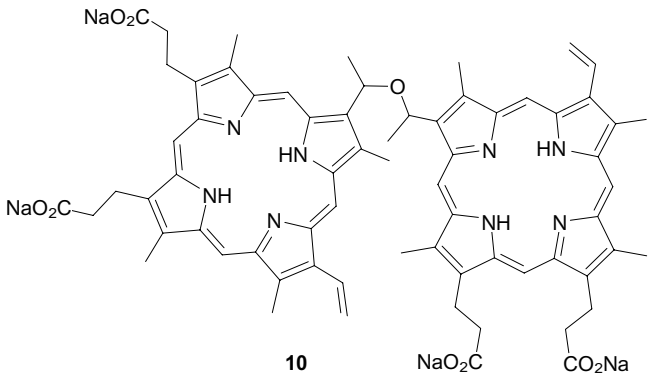


Structures 7 – 9



sodium (**10**), exhibits much higher activity (the therapeutic dose was decreased from 2.5 to 0.25 mg per kg of body weight), has good solubility in water and possesses low phototoxicity.

Structure 10



In the 1990s, second-generation PSs were developed. These PSs are based on hydrogenated porphyrins — chlorins and bacteriochlorins, phthalocyanines and their metal complexes.[37] Photosensitizers based on compounds of other classes, such as anthraquinones, cyanines, xanthenes and so on, are also known.[35, 38] Second-generation PSs have a rather intense absorption maximum at 660 – 670 nm, possess moderate cytophototoxicity, but are characterized by a rather low accumulation selectivity in tumour sites and, in some cases, poor solubility in water.

Among third-generation PSs (absorption maximum at 760 – 830 nm), mention should be made of extensively developed bacteriochlorophyll *a* derivatives and also the Pd bacteriochlorin complex Tookad (**8**, WST-11), which is already used in clinical therapy.[35, 39]

The experience of using PSs highlights the need for the development of new PSs for PDT of cancer with intense near-IR absorption and the necessity of replacing the currently used purely hydrophilic agents by amphiphilic PSs bearing bulky hydrophobic moieties. However, the efficient application of such PSs is possible only when using effective nanocarriers with desired characteristics.[29, 39] The most important characteristics are as follows:

1) good solubility of PS in water and the lack of tendency to aggregation;

2) the optimal particle size (150 – 200 nm) for passive accumulation in the tumour site due to passage through arteriovenous capillaries;

3) highly selective transport to target cells;

4) higher degree of phagocytosis of nanocarriers by target cells compared to the degree of their phagocytosis by cells of the reticuloendothelial system (RES) — the highest cell permeability was observed for particles with sizes of 30 – 300 nm;

5) stability during transport in the bloodstream and rapid biodegradation by lysosomal enzymes after target cell internalization and release of the unchanged drug;

6) inertness and non-immunogenecity for the body.

Hence, the ideal PS should be amphiphilic, *i.e.*, have a certain degree of hydrophilicity for easy administration to the body and a certain degree of hydrophobicity for the binding to target cells.

4. Main delivery vehicles for photosensitizers

4.1. Lipid-based nanoparticles

4.1.1. Liposomes

Lipid-based nanocarriers are the oldest and most commonly used PS delivery vehicles.[40] Liposomes are biodegradable nanoparticles, which have attracted attention of researchers due to their useful properties, such as controlled release, a versatile procedure for their preparation and high drug loading capacity.[41, 42] Liposomes are easily degraded in biological fluids, releasing PSs. The modification of the chemical structure of liposomes allows the encapsulation of PSs with different hydrophobicity, molecular weights, charges and acidity (basicity) constants.[43 – 45]

Depending on the materials used and preparation procedures, liposomes can encapsulate both hydrophobic and amphiphilic sensitizers and carry them to the target tumour site, the liposomes being easily biodegradable and cleared from the body.[46] Liposomes are closed spherical structures composed of a bilayer membrane. Their size varies from 50 nm to several micrometres. The liposome lipid bilayer generally consists of synthetic or natural phospholipids and cholesterol — structural components of cell membranes — and has a thickness of about 5 nm. Liposomes are characterized by structural diversity. Thus, they differ in the size, composition and the number of internal compartments.

Liposomes can be divided into two large groups — unilamellar and multilamellar. The former liposomes, with sizes of 20 – 100 nm, consist of one lipid bilayer, are not very stable, are easily degraded and rapidly release their content.

These liposomes are easily internalized by cells *via* endocytosis and can carry small amounts mainly of hydrophilic PSs. Multilamellar liposomes (with sizes of 100–5000 nm) include several lipid bilayers and are characterized by higher stability; they can carry both lipophilic (within the lipid bilayer of the liposome membrane) and hydrophilic PSs (in the internal compartment) in relatively small amounts.[47] Tumour capillaries rarely exceed 300 nm in diameter. Therefore, studies of nanosized delivery vehicles are focused on particles with sizes <200 nm (Fig. 3).

The efficiency of liposomal systems is related to their pharmacokinetics, which strongly depends on the size, surface charge, packing density of the lipid bilayer, steric stabilization, as well as on the dose and route of administration of the drug to the body. Important advantages of the application of liposomes as PS delivery carriers are a low degree of their aggregation and, as a consequence, high photodynamic efficacy. These nanostructures have the following drawbacks: low permeability of encapsulated PS due to the presence of cholesterol in liposomes, degradation of liposomes due to the exchange of lipids with high-density lipoproteins (HDL), the lack of target selectivity of standard liposomes and their uptake by normal cells, as well as opsonization of liposomes by plasma proteins, resulting in their rapid clearance from the blood circulation.[48,49]

The use of sterically stabilized liposomes (STEALTH®) makes it possible to substantially increase the half-life of these nanoparticles and to decrease the clearance rate through the reticuloendothelial system.[50,51] Polyethylene glycol (PEG) is the most commonly used polymeric stabilizing agent for liposomes. Polyethylene glycol is widely utilized in medicine due to good solubility in water, immunogenicity, lack of cytotoxicity and control by complement system proteins. Flexible PEG molecules create excess osmotic pressure in the near-membrane region of liposomes, due to which long-circulating vesicles are not recognized by RES.[52] Sterically stabilized liposomes have circulation half-lives of up to 45 h, as opposed to a few hours for standard liposomes. Nawalany *et al.*[53] reported the use of sterically stabilized PEGylated liposomes for delivery of two photosensitizers — 5,10,15,20-tetrakis(4-hydroxyphenyl)porphyrin (pTHPP) and its monosubstituted PEG conjugate with PEG molecular weight of 2000 Da (pTHPP-PEG2000) — to the human prostate adenocarcinoma cell line (DU-145) and the human colonic adenocarcinoma cell line (HCT-116). It was shown that the utilization of liposomes, as well as of substituted PEGylated porphyrin, leads to a considerable decrease in the dark cytotoxicity of PSs. Liposomes containing PSs proved to be more phototoxic compared with non-liposomal pTHPP-PEG2000. More recently, in 2012, this research group[54] prepared a series of PEGylated porphyrins with different PEG chain lengths (with molecular weights from 350 to 5000 Da) and evaluated PD activity of the liposomal formulation of these PSs. The attachment of PEG was found to decrease dark cytotoxicity of porphyrins in the DU-145 and HCT-116 cell lines. The phototoxicity of PEGylated porphyrins depends on the PEG chain length. The porphyrin–PEG conjugate with PEG molecular weight of 2000 Da exhibits the highest PD efficacy. The PS encapsulation in liposomes does not lead to a noticeable enhancement of the PD effect. Meanwhile, the liposomal formulation pTHPP-PEG2000 shows a tendency to induce apoptosis in both cell lines as opposed to PSs in solution.

New liposomes loaded with polyethyleneimine and sialic acid were prepared.[55] These liposomal formulations show a significant increase in the blood circulation half-life and they are not recognized by the reticuloendothelial system. In particular, polycationic liposomes for antiangiogenic PDT were studied. This procedure involves the vascular shutdown, reduced transport of nutrients and necrosis of tumour cells.[56]

In 2000, the medication Visudyne® was approved by the Food and Drug Administration (FDA) for sale in the United States as a drug for the treatment of age-related macular degeneration, which significantly impairs vision; in 2001, it was approved for the treatment of pathologic myopia. Visudyne is a lyophilized liposomal formulation

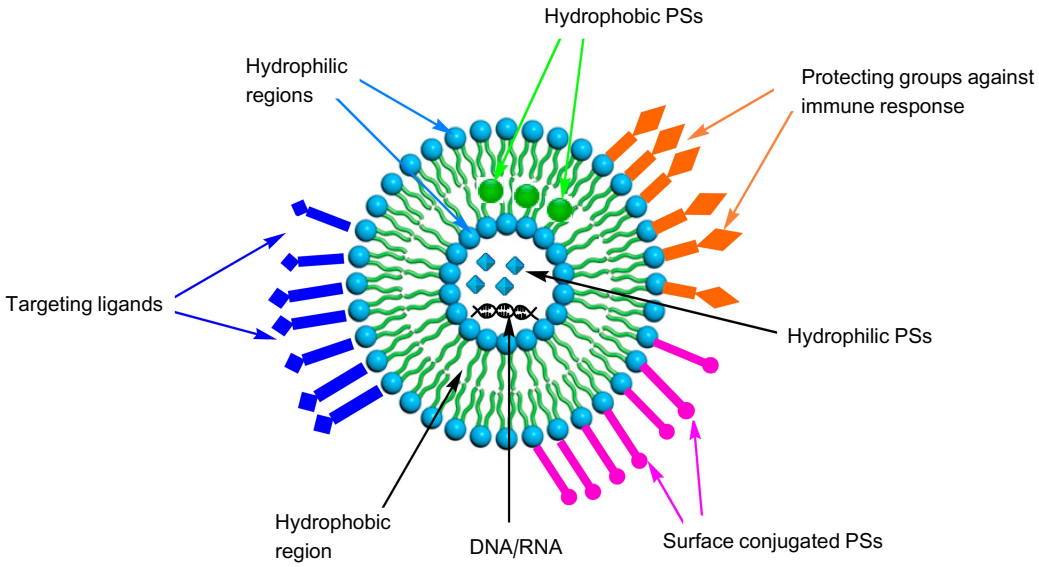


Figure 3. Schematic representation of photosensitizers (PS) entrapped in the hydrophobic or hydrophilic regions of a liposome.[40]

of the second-generation PS Verteporfin. The drug consists of zwitterionic dimyristoyl phosphatidylcholine (DMPC), negatively charged egg phosphatidylglycerol and hydrophobic Verteporfin derived from protoporphyrin IX.[57] Visudyne reduces the risk of loss of vision caused by age-related macular degeneration in patients with predominantly classic or repeated subfoveal choroidal neovascularization secondary to pathological myopia.[58] This disease is characterized by an increase in the level of vascular endothelial growth factor (VEGF) in internal eye structures, which leads, during the natural development, to the formation of a fibrovascular scar and irreversible central blindness. The pharmacokinetics of this drug was improved by the surface modification of liposomes with different substances, such as polyethylene glycol, antibodies, peptides, folic acid and so on.[59–61]

Lassalle's research group[62] developed the liposomal formulation Foslip consisting of a mixture of dipalmitoylphosphatidylcholine (DPPC), dipalmitoyl phosphatidylglycerol (DPPG) and 5,10,15,20-tetrakis(3-hydroxyphenyl)chlorin (Foscan®, mTHPC) as the PS. This drug was assayed *in vivo* in the mouse tumour cells EMT6, which showed that, after the intravenous administration of this drug at a dose of 0.3 mg kg^{-1}, the volume of distribution was four times larger compared with the administration only of PS (709 *versus* 172 ml kg^{-1}).[63] The maximum accumulation of mTHPC in the tumour was achieved in 72 h; in the case of Foscan®, 24–48 h after the administration. After 6 h, PS was present both in the vascular system and cancer cells. Foslip liposomes show a slower release of mTHPC compared to Visudyne liposomes consisting of more liquid lipids.

Fospeg® is another liposomal formulation of mTHPC, which was developed to increase its stability, half-life and circulation time. Besides, these liposomes contain a PEG.[64] This formulation is characterized by lower dark cytotoxicity and higher therapeutic efficacy. The same research team[65] performed a comparative study of two liposomal formulations of mTHPC — Fospeg and Foslip. The dependence of PDT efficacy on the following parameters was evaluated: pharmacokinetics, PS release, stability of liposomes, tumour tropicity and intracellular distribution in the tumour. Fospeg proved to be a more effective formulation of mTHPC compared to Foslip, because it has greater cellular permeability, higher accumulation in the tumour and higher stability in blood circulation. The most essential advantage of Fospeg is a considerable decrease in the time interval between PS administration and laser activation. Gaio *et al.*[66] compared the phototoxicity of Foscan and its liposomal formulations — Foslip and Fospeg — in HeLa tumour cell spheroids. The application of the liposomal formulations was shown to increase accumulation of PS, significantly abolish dark cytotoxicity and promote spheroid disassembling to a higher extent when compared to Foscan.

The liposomal formulation of Photofrin shows much higher activity in the human glioma model implanted into the rat brain compared to the starting Photofrin. Significant *in vivo* cellular uptake of the liposomal formulation was observed in tumour tissues of the 9L gliosarcoma model in rats and the U87 glioma model in nude mice.[67,68] The encapsulation of Foscan in multilamellar liposomes also increases its therapeutic efficacy in mice implanted with a human gastric cancer xenograft.[69]

Biodegradable nanoemulsions of Foscan were described by Primo *et al.*[70] A nanoemulsion of mTHPC in a mixture of soybean phosphatidylcholine (PC), soybean lecithin (Epikuron 170), a polysorbate (Tween 80) and non-ionic surfactants was prepared by a standard procedure from an aqueous medium and an organic phase composed of non-ionic surfactants. It was shown that the photophysical properties of PS remained unchanged after its incorporation into the nanoemulsion. The *in vitro* assay was performed using mimetic biological environment protocols based on an animal model. The nanoemulsion of Foscan was detected in different skin layers 6 h after topical administration, and the Foscan diffusion flux was shown to be higher compared to its diffusion in physiological medium.

5-Aminolevulinic acid (ALA) is widely used in PDT because it is metabolized into protoporphyrin IX in the body. However, ALA has poor tissue permeability. The ALA loading in liposomes composed of phosphatidylethanolamine, cholesterol and sodium stearate in a ratio of 2 : 1 : 2.5 leads to an increase in ALA accumulation in the tumour by 29%.[71]

Shim *et al.*[72] reported the preparation of cationic nanolipoplexes based on chlorin e_6 (Chl-e_6) and 1,2-dioleoyl-*sn*-glycero-3-ethylphosphocholine. The uptake of Chl-e_6-loaded lipoplexes by SCC7 tumour cells was 18.3 higher than that to free chlorin. The molecular imaging revealed the preferential distribution and retention of Chl-e_6 in SCC7 tumour tissues after intravenous administration of Chl-e_6 in cationic nanolipoplexes. Moreover, the local illumination of mice that received Chl-e_6 in cationic nanolipoplexes resulted in complete degradation of the tumour compared with the group of animals treated with free chlorin, which showed continuous tumour growth.

Recently, a Chinese research group[73] performed a study aimed at reducing side effects associated with the accumulation of Chl-e_6 in normal tissues, especially in skin. Apart from chlorin, phospholipid-based liposomes were loaded with the dye indocyanine green (ICG), which was approved for clinical applications in 1959. After exposure of these liposomes to laser radiation at 660 nm, Chl-e_6 does not generate singlet oxygen, because the energy of excited PS is absorbed by ICG. However, after laser irradiation first at 808 nm and then at 660 nm, the fluorescence of Chl-e_6 was recovered. This is because irradiation at 808 nm causes ICG degradation and the energy of excited chlorin can again be transferred to oxygen. The authors described this effect as turning 'ON' and 'OFF' the photosensitizer. Both processes can be monitored by measuring the fluorescence intensity of Chl-e_6: the maximum intensity is observed when Chl-e_6 is turned 'ON', and it decreases almost to zero when Chl-e_6 is turned 'OFF'. The efficiency of this method was demonstrated in *in vitro* experiments. It should be noted that, apart from PDT, additional cancer cell destruction was induced by the photothermal effect associated with the ICG degradation upon irradiation at 808 nm (Fig. 4).

Przybylo *et al.*[74] studied the influence of protoporphyrin IX-loaded liposomes of different compositions on the efficacy of delivery of PSs and their distribution in the cell. In order to evaluate the efficacy of delivery, liposomes were labelled with the fluorescent dye 6-{[*N*-(7-nitrobenz-2-oxa-1,3-diazol-4-yl)amino]hexanoyl}sphingosine (NBD-C6), and the PS delivery was assessed based on the intrinsic fluorescence of the dye. The imaging selectivity was achieved by using different excitation wavelengths: 405 nm

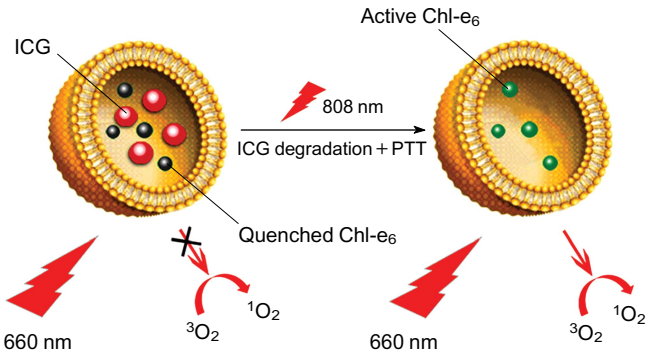


Figure 4. Mechanism of action of the chlorin e_6–indocyanine green system (ICG).[73] PTT is photothermal therapy.

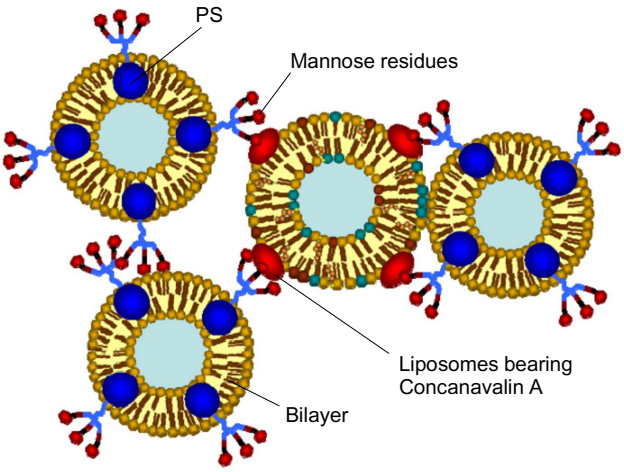


Figure 5. Structure of photosensitizers (PS) and their aggregates.[77]

for PS and 488 nm for NBD-C6. Both charged and neutral liposomes of different compositions were prepared. Neutral and anionic liposomes were most efficiently internalized by HeLa cancer cells. It was shown that all intracellular structures, except the nucleus, were intensely coloured by the fluorescent dye, which attests to the efficient uptake of these liposomes by the cell.

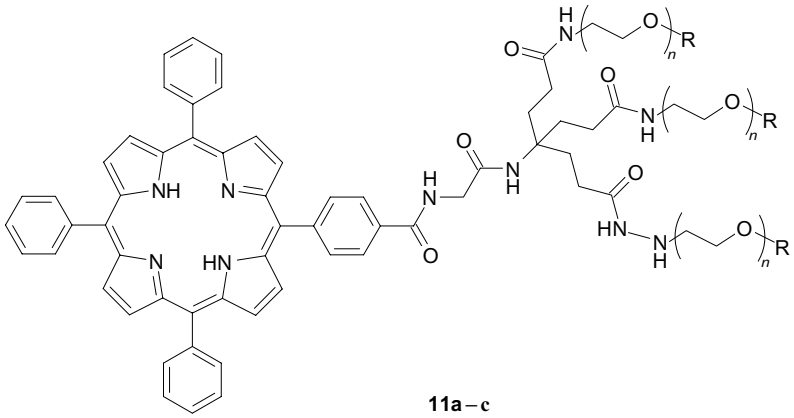
Maillard and co-workers[75–78] synthesized glycodendrimeric porphyrins **11a–c** as promising drugs for the treatment of retinoblastoma.

It is known that mannose receptors are overexpressed on the surface of retinoblastoma cells. In view of this fact, this research group built original biomimetic membranes and supported planar bilayers, which have a composition similar to that of the retina and bear the mannose-specific protein Concanavalin A, and studied the interaction of these membranes with synthetic glycodendrimeric porphyrins (Fig. 5). Only mannosylated porphyrins were found to interact with a model membrane. This procedure can be used to find potentially active compounds.

In recent years, self-assembled liposome-like structures, namely, nanocells and porphysomes, have attracted great interest.[79] Nanocells are constructs, in which PSs are trapped inside polymeric nanoparticles and the latter are then encapsulated in PEGylated liposomes. Porphysomes are covalent porphyrin–phospholipid conjugates self-assembled to liposome-like nanoparticles. These nanosystems are biodegradable nontoxic vesicles about 100 nm in diameter. In addition to a bilayer structure, porphysomes have unique photophysical characteristics, such as the variability in extinction coefficient, structure-dependent fluorescence quenching and unique photothermal and photoacoustic properties. Porphysomes exhibit good stability and can be stored for months in aqueous media, but they undergo enzymatic degradation. The vesicular structure of porphysomes is disrupted upon incubation with lipase or detergents (surfactants). Porphysomes are characterized by an extremely high packing density of porphyrins (> 80 000 per particle), which leads to their self-quenching. At certain time points, porphysomes can mediate photoacoustic and photothermal effects. In *in vivo* conditions, molecules dissociate and the released monomeric PSs are actively involved in PDT.

Lovell's research group[80–83] studied porphysomes based on 2-(1-hexyloxyethyl)-2-devinyl pyropheophorbide **7** conjugated to lysophosphatidylcholine and loaded with Doxorubicin. Porphysomes were used to release Doxorubicin from leaky liposomes and subsequent vascular-targeted PDT involving PS.[84] *In vitro* and *in vivo* studies of porphysomes with 5 molar % HPPH and Doxorubicin showed that these liposomes are stable in the blood serum. It was also found that a higher load of HPPH leads to destabilization of liposomes. Near-infrared laser irradiation induced vas-

Structures 11



11a–c

a: n = 2, R = H;
b: n = 2, R is α-mannosyl;
c: n = 3, R is α-mannosyl

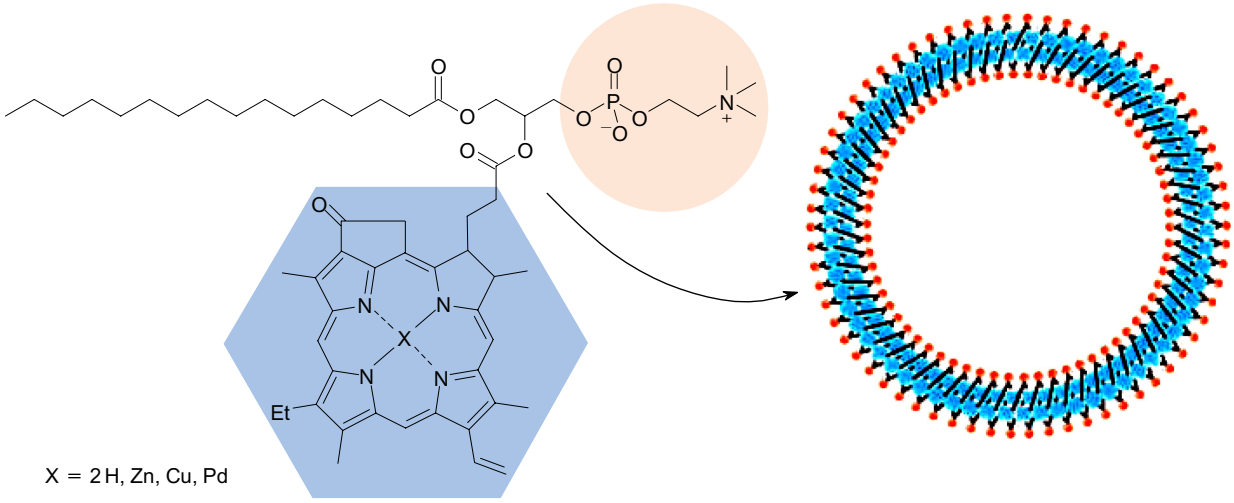


Figure 6. Structure of porphysomes.[85]

cular photodynamic damage and the Doxorubicin accumulation in the tumour. The utilization of such leaky HPPH liposomes leads to a substantial improvement of Doxorubicin bioavailability. These assays were performed in nude mice bearing KB or MIA Paca-2 xenografts.

More recently, porphysomes were suggested as photonic porphyrin shell microbubbles (Fig. 6). The investigation of their acoustic and photoacoustic properties led to the conclusion that these porphysomes are suitable for both ultrasound and photoacoustic imaging of biological specimens with a resonance frequency of 9–10 Hz.[85,86] This research group[87] also developed folic acid-modified porphysomes. The efficiency of these two types of porphysomes was compared in *in vitro* experiments. It was shown that folate-targeted porphysomes exhibit much higher cellular uptake.

The conjugation of metal complexes of synthetic chlorins to lipids resulted in the formation of nanovesicles, which can be used as biophotonic contrast agents for photoacoustic and fluorescence imaging and photothermal therapy (Fig. 7).[88] The authors of this study modified pyropheophorbide *a* by introducing the methoxymethyl group at the 3 position, incorporating a zinc ion into the macrocycle and attaching lipid to a propionic acid moiety. The electronic absorption spectrum of this conjugate shows a strong bathochromic shift of the Q band (72 nm), along with an increase in absorbance and circular dichroism.

An alternative strategy for increasing the efficacy of liposomal anticancer agents is based on the attachment of vector molecules to the liposome surface. Monoclonal antibodies, peptides, glycoproteins, oligonucleotide aptamers, polysaccharides, as well as ligands specific for different types of cancer (*e.g.*, folic acid, growth factor, transferrin, cholesterol), are used for this purpose.[89–91]

The application of liposomes combined with different endogenous (pH, enzymes) and exogenous (irradiation, temperature, ultrasound) stimuli has attracted considerable interest. These are so-called triggerable liposomes, which are based on the response to an external trigger, resulting in the degradation of the liposomal membrane and PS release in the tumour tissue.[92–94] The utilization of such liposomes

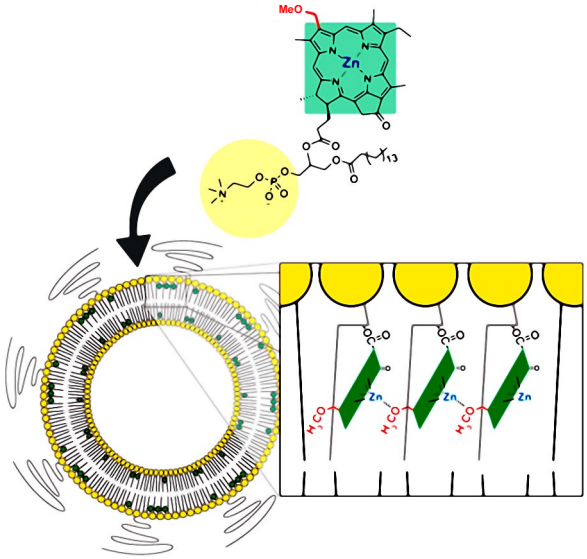


Figure 7. Structure of metallochlorin–llipid conjugate.[88]

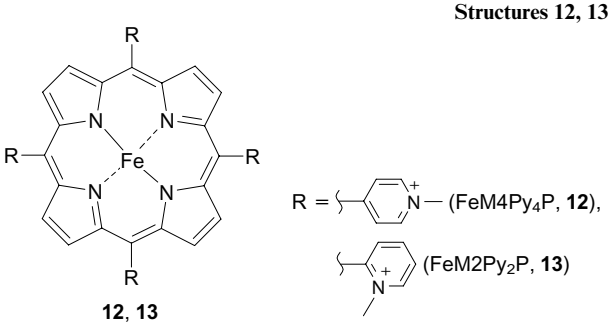
leads to an increase in the PS accumulation in the tumour and diminishes non-specific light sensitivity of normal tissues. Thermosensitive liposomes contain specific lipids, which are composed of phospholipids with a phase transition temperature higher than the body temperature (*e.g.*, DPPC) or bear thermosensitive polymers on the surface. These liposomes undergo a gel-to-liquid crystalline phase transition at >42 °C. At this temperature, the phospholipid bilayer has higher permeability. In the body, these liposomes are stable, but the local heating at >42 °C leads to drug release.[95]

Tan *et al.*[96] developed thermosensitive liposomes containing Chl-e_6 and folic acid. The authors combined the photodynamic effect of PS and the photothermal (PT) effect of copper sulfide (CuS). The mechanism of action of these liposomes is as follows. First, cancer cells are irradiated with 808 nm laser, thereby inducing the PT effect of

copper(II) sulfide encapsulated in liposomes and causing both cell death and degradation of thermosensitive liposomes. Then PS is released upon 660 nm laser irradiation to kill cancer cells. A combination of these two methods in *in vivo* experiments showed significant inhibition of tumour growth without noticeable adverse effects.

Another strategy is based on the surface modification of liposomes by pH-responsive molecules, *e.g.*, phosphatidylethanolamine (PE). The latter stabilizes the membrane at neutral pH and causes degradation of liposomes in the tumour cell-conditioned medium with pH 6.5–6.8. Thus, pH-responsive liposomes were prepared based on Fe complexes of cationic porphyrins $FeM4Py_4P$ (**12**) and $FeM2Py_2P$ (**13**), 1,2-dimyristoyl-*sn*-glycero-3-phosphatidylcholine, dimethyldidecylammonium bromide (DDAB), sodium oleate and the non-ionic surfactant polysorbate 80.[97]

Structures 12, 13



12, **13**

Earlier, water-soluble Fe complexes of cationic porphyrins were studied as superoxide dismutase (SOD) biomimetics.[98] The low SOD activity in cancer cells leads to an increase in the amount of intracellular free-radical oxygen. Reactive oxygen species, such as the $O_2^{-\bullet}$ radical anion or hydrogen peroxide (H_2O_2), are essential cell death regulators. The effect of some anticancer drugs is based on activation of ROS in cells. Iron porphyrins complexes are considered as SOD mimics, controlling the levels of $O_2^{-\bullet}$ and H_2O_2 in cancer cells. Thus, the $O_2^{-\bullet}$ radical anion undergoes enzymatic transformation into H_2O_2 induced by porphyrin. The efficiency of this process is associated with the presence of PS in the bloodstream. In order to increase the circulation time, Yuasa *et al.*[99] attached water-soluble positively charged 5,10,15,20-tetrakis[*N*-methyl-2(4)-pyridinio]porphyrin to the outer surface of liposomes *via* electrostatic interactions and adsorption of sodium oleate. These liposomes release an iron porphyrin complex at low pH values.

The antigen-mediated liposome transport is also a promising approach to targeted PDT.[100,101] The conjugation of liposomes to appropriate vectors allows the modulation of liposome distribution in tissues and organs. The immunoliposome delivery is targeted by monoclonal antibodies (mAbs) against tumour-specific antigens. At the present time, 76 antibodies targeted to anticancer antigens have been approved by FDA.[102] Immunoliposomes bearing pheophorbide *a*,[103] benzoporphyrin derivatives,[104] indocyanine green,[105] AlCl phthalocyanine[106] and tetraphenylporphyrin (TPP)[107] were developed.

Photoactivatable liposomes loaded with benzoporphyrin and bearing the mAb Bevacizumab (Avastin®) were prepared.[108] This mAb selectively binds to vascular endothelial growth factor (VEGF), which is a key proangiogenic factor, and inhibits VEGF activity. This antibody is used because of high incidence of tumour recurrence even after systemic chemotherapy. Such liposomes enhance inter- and intracellular drug delivery and increase *in vitro* acute cytotoxicity. *In vivo* studies of pancreatic ductal adenocarcinoma in mice showed that the use of these liposomes leads to a significant decrease in the tumour size. This effect is related to the optimal PS content in liposomes and is possible due to the efficient inhibition of VEGF by Bevacizumab.

Folate-conjugated liposomes bearing a Zn TPP complex were used for targeting to HeLa cancer cells overexpressing folate receptors.[109] At a Zn TPP concentration of 1 μmol litre^{-1} and irradiation with 10 J cm^{-2}, non-targeted liposomes cause 65% cell death in the HeLa cell line, while folate-targeted liposomes induce 94% cell death. Liposomes containing Verteporfin and bearing antibodies against epidermal growth factor receptor (EGFR) were proposed for the treatment of ovarian carcinoma.[104,110] Cancer cells treated with these liposomes were shown to have lower viability compared to those treated with standard liposomes. Most principles applicable to immunoliposomes can also be used for the preparation of liposomes modified with other ligands.

The wide application of immunoliposomes is limited by high cost of antibodies;[111] however, the targeting effect of these nanostructures is high. Table 1 summarizes known data on the use of liposomal formulations in clinic and on the agents that are in different stages of biological trials.

In the past decade, an alternative colloidal delivery system for hydrophobic drugs, namely, solid lipid nanoparticles (SLNP) composed of high-melting triglycerides or other lipid substances, has been extensively studied.[112] These constructs combine advantages of different colloidal nanoparticles, for example, physical stability, protection of labile drug substances (DS) from degradation, controlled drug release, excellent drug tolerance, site-specific targeting. The drawbacks are the limited DS loading capacity and drug leakage during long-term storage. These nanoparticles are aqueous colloidal dispersions, the matrix of which comprises solid biodegradable lipids.[113] Navarro *et al.*[114] showed that mTHPC was efficiently incorporated into the lipid core of SLNP. The nanoparticles thus prepared were stable within six months and had a rather narrow particle size distribution. Phototoxicity was evaluated in MCF-7 cells upon irradiation at 652 nm with a range of light fluence from 1 to 10 J cm^{-2}. It was shown that lipid nanoparticles used at high concentrations have a cytotoxic effect. Hence, the authors designed a formulation containing a high PS concentration (230 mTHPC molecules per nanoparticle). Photodynamic efficacy of mTHPC-loaded nanoparticles proved to be statistically significant compared with naked SLNPs (Fig. 8).

4.1.2. Micelles

Micelles are formed by self-assembly of surfactant molecules, where hydrophilic regions are in contact with solvent molecules, while the hydrophobic tails form the central core. The particle size varies from 5 to 100 nm. Micelles can be divided into polymeric and lipid micelles depending on the structure of the amphiphilic core (Fig. 9). Polymeric micelles are composed of block copolymers, whereas lipid micelles consist of conjugates of water-soluble polymers with lipids. The self-assembly of amphiphilic block copolymers in water is based on nonpolar and hydrophobic

Table 1. Lipid nanoparticles for photodynamic therapy.

Photosensitizer	Type of nanomaterial	Investigation stage	Applications	Ref.
Verteporfin (Visudyne) (semisynthetic chlorin, protoporphyrin IX derivative)	Liposomal formulation	Clinic	Widely used in ophthalmology as a PS combined with a transpupillary red laser for the treatment of age-related macular degeneration	57–59
	The same	*In vivo*	Combination of Verteporfin and immunosuppressive agents shows the potential of PDT for the treatment of inflammatory subfoveal choroidal neovascularization (CNV)	60
	"	*In vivo*	Destruction of tumour-associated lymphatic vessels	61
Foslip (mTHCP)	DPPC/DPPG Liposomal formulation	*In vivo*	Used as a PS in a mouse model of local breast cancer recurrence; has photothrombic activity	62, 63
Liposomal Photofrin	Unilamellar DPPC vesicles	*In vivo*	Increased uptake of Photofrin by tumours after PDT; prevents Photofrin aggregation	67, 68
	Multilamellar liposomes	*In vivo*	High apoptosis index of tumour tissue after PDT	69
Foscan nanoemulsions	Emulsion of mTHPC in soybean PC, an Epikuron 170–Tween 80 mixture and non-ionic surfactants	*In vitro*	Application of a Foscan nanoemulsion for skin and mucosa in PDT of skin cancer	70
Lipoplexes bearing negatively charged chlorin e6	Cationic lipoplexes	*In vivo*	Selective tumour targeting and improvement of the therapeutic effect on the tumour after PDT compared to standard Chl-e_6	72
Porphysome nanovesicles	Self-assembled lipid-conjugated tetrapyrrole PS	*In vitro*	Multimodal potential; enables visualization of lymphatic systems by photoacoustic imaging; are accumulated in tumours of mice bearing xenografts; laser irradiation causes photothermal tumour destruction	80–84
Tetraphenylporphirin (TPP)	Phosphatidylethanolamine (PEA) micelles were modified by tumour-specific mAb 2C5	*In vivo*	An improved anticancer effect after PDT for murine Lewis lung carcinoma was demonstrated	107

interactions between lipophilic polymer chains, which form the core of micelles.

Lipid micelles consist of PSs and phospholipids covalently or noncovalently bonded to each other. In some cases, these micelles can contain polymers, such as PEG (Fig. 10).[115] A delivery system of this type was proposed for Chl-e_6.[116] Nanospheres fabricated by lipopolymers in different ratios and comprising phosphatidylcholine, pH-responsive phosphatidylethanolamine-poly(l-histidine) and thermosensitive phosphatidylethanolamine-poly(*N*-isopropylacrylamide) are characterized by long blood circulation time, stable particle size of about 100 nm, positive surface charge, low cytotoxicity and Chl-e_6 loading capacity of up to ~45%. These nanospheres show considerable photodynamic therapeutic efficacy in KB cancer cells compared to free chlorin.

A method was developed for the preparation of micelles based on derivatives in which the lipophilic cholesterol moiety (either hexadecyl- or cholest-5-en-3β-yloxyethyl) is bound to the 13^1, 15^2 and 17^3 positions of the chlorin macrocycle.[117] These conjugates were mixed with egg-yolk PC to form micelles stable under physiological conditions. These micelles were found to bind to human MCF-7 breast carcinoma cells.

Tachikawa *et al.*[118] attached higher alkyl chains (C_{13}–C_{17}) to protoporphyrin IX (Proto IX). In water,

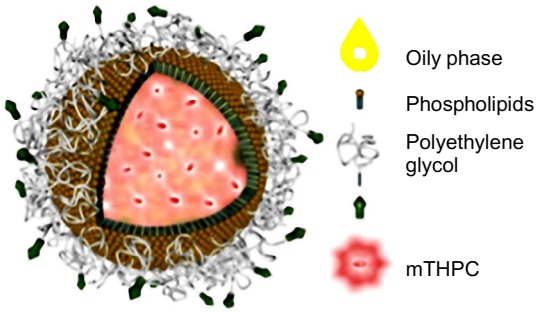


Figure 8. Schematic of *meso*-tetra(hydroxyphenyl)chlorin (mTHPC)-loaded lipid nanoparticles.[114]

these compounds formed micelles exhibiting low cytotoxicity toward HeLa cells (the half-maximal inhibitory concentration (IC_{50}) was in the range of 151.7–379.9 μmol litre^{-1}). Besides, this research team prepared liposomes by the post-insertion of Proto IX micelles into liposomes composed of distearoylphosphatidylcholine, cholesterol and modified PEG — distearoylphosphatidylethanolamine–PEG2000. The photodynamic effect of both micelles and liposomes proved to be ten times weaker than

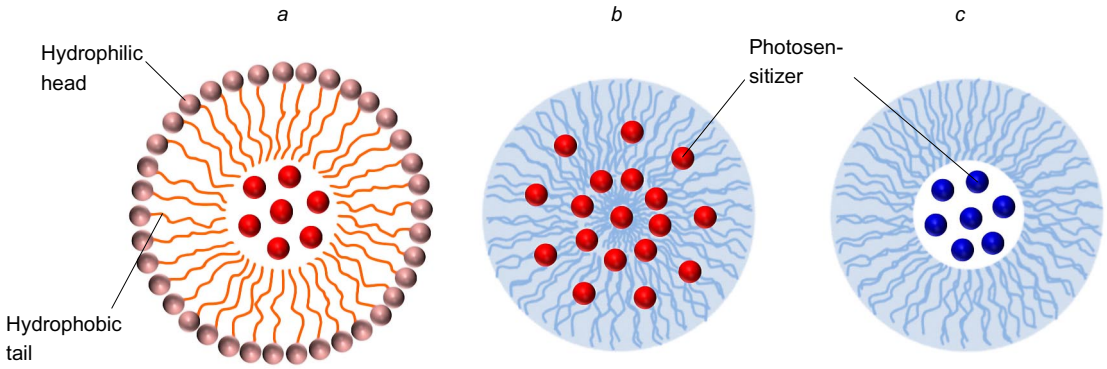


Figure 9. Schematics of polymeric particles: micelles (*a*), nanospheres (*b*) and nanocapsules (*c*).[38]

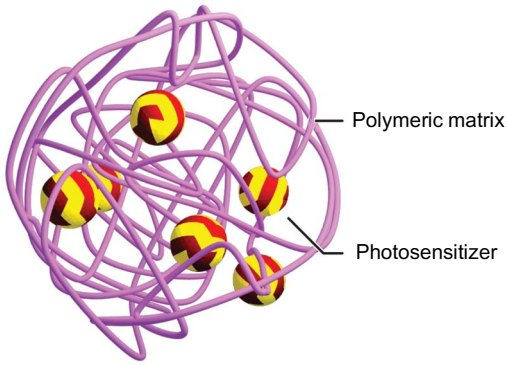


Figure 10. Lipid micelle with sizes of 30–122 nm.[115]

that of protoporphyrin IX. It was also found that liposomes containing the heptadecyl substituent (PL-C17) selectively accumulated in the Golgi apparatus, which can be further used in combined PDT with viral adjuvants based on these liposomes.[119]

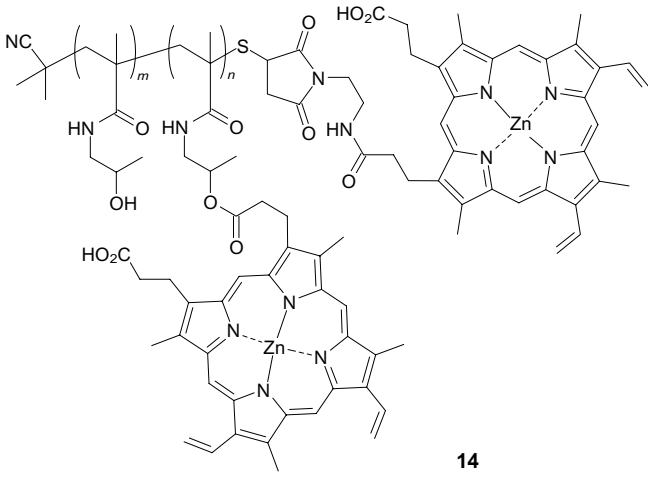
Polymeric micelles self-assembled in water from amphiphilic polymers at the critical micelle concentration.[120] These micelles have a hydrophobic core formed by hydrophobic polymer fragments and an outer shell formed by hydrophilic segments (normally PEG). The shell allows micelles to circulate in the bloodstream for long periods.[121] An example of such micelles is Pluronic PEG-PPO-PEG composed of one hydrophobic polypropylene oxide (PPO) segment flanked by two PEG segments. It exists in two forms — P123 and F127. Only the P123–F127 binary system in a ratio of 2:1 was found to entrap the photosensitizer Verteporfin in the monomeric form. This formulation has much higher phototoxicity in *in vitro* assays compared to the starting PS.[122]

Photodynamic activity of Pluronic P123/F127 mixed polymeric micelles loaded with Photofrin II® was evaluated in human MCF-7/WT breast cancer cells (caspase-3 deficient) and SKOV-3 ovarian cancer cells (resistant to chemotherapy).[123] The most interesting results were obtained in SKOV-3 cells resistant to cisplatin, adriamycin, diphtheria toxin, *etc*. Roby *et al.*[124] reported the preparation of polymeric micelles composed of the PEG–phosphatidylethanolamine conjugate and showed that these micelles efficiently solubilize TPP. This PS proved to be efficient *in vitro* against the mouse cancer cell line (LLC) and human breast cancer cell lines (MCF-7, BT20). The surface modification of TPP-loaded micelles with the tumour-specific monoclonal antibody 2C5 substantially enhances cancer cell death compared to standard micelles. In 2007, this research group[107] studied immunomicelles *in vivo* in mouse carcinoma LLC cells. Immunomicelles showed the maximum tumour growth inhibition.

Nakamura *et al.*[125] synthesized *N*-(2-hydroxypropyl)methacrylamide polymer conjugated with the zinc protoporphyrin IX complex and evaluated its application for the tumour detection by *in vivo* imaging and treatment using the mouse S-180 sarcoma model. Conjugate **14** spontaneously formed micelles in aqueous medium. The hydrophobic core of these micelles consisted of protoporphyrin, and the shell was composed of the hydrophilic polymer. The hydrodynamic diameter of these micelles was 82.8 ± 4.8 nm. This conjugate had a plasma half-life markedly longer (more than 40 times) than that of free protoporphyrin and selectively accumulated in tumour tissues (10 times more in the tumour than in the lung, kidneys and heart).

Koo *et al.*[126] described protoporphyrin IX-encapsulated pH-responsive polyethylene glycol–poly(β-amino ester) polymeric micelles. The uptake of these micelles by the RES was found to be low. A tenfold increase in the accumulation of micellar nanostructures was observed in SCC7 tumour-bearing mice after 48 h. The histological examination showed that most tumour cells in mice treated

Structure 14



14

with protoporphyrin IX-encapsulated micelles were severely damaged or destroyed 10 days after the treatment, whereas there was incomplete cancer cell death in mice treated with free PS.

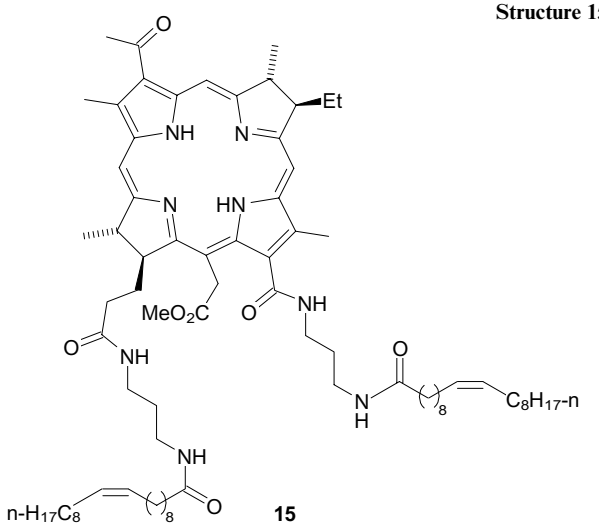
Approaches to the combined treatment of tumours using chemotherapy and PDT were proposed in the studies.[127, 128] For this purpose, Wang *et al.*[128] prepared the pH-responsive diblock copolymer PEG-block-poly(2-diisopropylamino)ethyl methacrylate-*co*-(2-hydroxylethyl)methacrylate, which self-assembled into micelles at neutral pH (> 6.3), incorporating Chl-e_6, gadolinium(III) ions and a Pluronic prodrug of Doxorubicin. In this system, Chl-e_6 and Gd^{3+} were inactivated at neutral pH (*i.e.*, in the bloodstream), but became highly active in acidic tumour microenvironment and generated fluorescence and a NMR signal for visualization by MRI. This system enhanced cytotoxicity of Doxorubicin, and Chl-e_6 actively generated singlet oxygen.

4.2. Lipoprotein-based nanostructures

Lipoproteins (LPs) represent another class of nanoparticles used in PDT.[129] These nanoparticles consist of a hydrophobic core, which is composed of cholesterol esters and triglycerides, and a shell formed by specific apoproteins, phospholipids and cholesterol. The hydrophobic nature of the core facilitates the incorporation of hydrophobic PSs. Taking into account that many malignant tumours overexpress LP receptors on the surface of cancer cells,[130] the incorporation of PSs into low-density lipoproteins was studied for such PSs as phthalocyanines,[131] benzoporphyrin derivaties[132] and tetraphenylporphyrin derivatives.[133] The loading of mono-, di- and tetrasulfonated tetraphenylporphyrins into LDLs and their delivery to the tumour were studied by Kessel *et al.*[134] The number of polar groups was found to strongly influence the interaction with LDLs, disulfo derivatives being most active. Low-density lipoprotein-based nanoparticles loaded with benzoporphyrin as PS were used in assays in rabbits transplanted with choroidal melanoma. Fast thrombosis followed by tumour necrosis were observed during PDT.

The third-generation photosensitizer — bacteriochlorin e_6 bisoleate (Bchl-BOA, **15**) — encapsulated into high-density lipoproteins (HDL) showed high photoactivity in nude mice bearing human HepG2 liver carcinoma.[135, 136] Photodynamic therapy with bacteriochlorin e_6–LDL nanoparticles prevents tumour volume doubling in theses mice for 60 days after PDT. The control animals experience tumour volume doubling within 12 days.

Structure 15



15

Cui *et al.*[137] synthesized porphyrin–lipoprotein nanostructures for positron emission tomography (PET) and near-IR imaging. These nanostructures have a hydrophobic lipid–porphyrin core surrounded by ApoA-1 mimetic peptide R4F (Ac-FAEKFKEAVKDYFAKFWD). The clinically relevant glioblastoma model enabled delineation of the tumour from surrounding healthy brain cells with exceptionally high precision (up to 1 nm). Hence, this approach holds great promise for intraoperative fluorescence-guided surgery and tumour-selective PDT.

4.3. Polymeric nanoparticles

Polymeric nanoparticles (PNPs) are attractive PS delivery vehicles due to high stability, relatively small diameter and narrow size distribution. A small size reduces macrophage recognition of PNPs and increases their blood circulation time. Both synthetic polymers, such as polylactide (PLA), polyglycolide (PGA), poly(lactide-*co*-glycolide) (PLGA), polyacrylamide, *N*-(2-hydroxypropyl)methacrylamide, *etc.*, and natural polymers, *e.g.*, chitosan, albumin and collagen,[138–143] hold considerable promise. The surface of PNPs can be modified by specific ligands for active targeting.[144] The controlled release of encapsulated PSs from a polymeric carrier is driven by the polymer degradation under physiological conditions, diffusion of the drug substance through the polymeric matrix and structural changes of the polymer in response to characteristics of the cellular microenvironment, *e.g.*, pH, temperature, the presence of specific enzymes.[39, 145–147] There are several physicochemical mechanisms of PS release from polymeric nanoparticles:[39]

1) enzymatic polymer degradation at the delivery site, resulting in PS release;

2) swelling of polymeric nanoparticles due to hydration, the influence of pH and temperature and subsequent PS release through diffusion;

3) release of the drug substance from the polymer.

Hydrophobic PSs can be incorporated into the core of PNPs through hydrophobic or electrostatic interactions. The size of these nanoparticles is controlled by varying the composition of the polymers. Biodegradable polymers, such as polyacrylamide (PAA), PLA, PGA, polycaprolactone (PCL) and also their copolymers, are most commonly utilized for the preparation of nanoparticles. Polylactide, polyglycolide and their copolymer — poly(lactide-*co*-glycolide) (PLGA) — are widely used due to physical stability, biocompatibility, high drug loading capacity and controllable drug release. Poly(lactide-*co*-glycolide) was approved by the FDA for the use as a drug delivery vehicle.[148]

Nanoparticles of PLGA are synthesized by copolymerization of cyclic dimers of lactic and glycolic acids giving nanospheres. The copolymers can have different masses and structures, which makes it possible to vary the degree of interaction between macromolecules and the biodegradation rate of particles. Besides, polyethylene glycol-coated PLGA nanoparticles showed high resistance to hydrolysis in culture medium (in the protein environment) and prolonged blood circulation time.[149] In the body, PLGA nanoparticles undergo hydrolysis to form lactic and glycolic acids, which are eliminated from the body *via* the Krebs cycle.

Ogawara *et al.*[150] incorporated hydrophobic Proto IX into polymeric nanoparticles composed of the PEG–PLA

block copolymer. The average size of loaded nanoparticles was about 80 nm. The zeta potential was determined to be slightly negative. The *in vitro* phototoxicity assay showed that these nanoparticles are highly phototoxic to three types of tumour cells [Colon-26 carcinoma (C26), B16BL6 melanoma and Lewis lung cancer cells] depending on the concentration of Proto IX nanoparticles. *In vivo* pharmacokinetics of these nanoparticles after the intravenous administration was evaluated in C26 tumour-bearing mice. Nanoparticles exhibited low affinity to the liver and spleen and were therefore retained in the blood circulation for a long time. Furthermore, significant antitumour effect was observed in C26 tumour-bearing mice after local irradiation.

The copolymerization of polymers with polyethylene glycol is used to increase the solubility of hydrophobic polymers and improve loading capacity for hydrophilic drugs. Polyethylene glycol not only improves hydrophilicity and drug loading but also increases the *in vivo* circulation time and protects nanoparticles from being engulfed by macrophages.[151] Cohen *et al.*[152] synthesized the PEG–PLA block copolymer by ring-opening polymerization. These nanoparticles were utilized for the delivery of 5,10,15,20-tetrakis(3-hydroxyphenyl)porphyrin to head and neck cancer cells (HSC-3 and HN-5). A higher mTHPP loading led to enhancement of cellular fluorescence and dark cytotoxicity. In general, 2% mTHPP micelles are optimal for PDT. Pramual *et al.*[153] used new hybrid nanoparticles for the delivery of 5,10,15,20-tetrakis(4-hydroxyphenyl)porphyrin (pTHPP). The nanoparticle core consisted of PLGA and poly(hydroxybutyrate-*co*-hydroxyvalerate) (PHBV), and the shell was composed of carboxy(polyethylene glycol) 2000 mixed with lecithin. The concentration of PS loaded in nanoparticles was 5%, 10% and 15%. The resulting nanoparticles had an average size of 88.5 ± 3.4 nm. They ensured efficient singlet oxygen generation and active cellular uptake in human FTC-133 carcinoma cells.

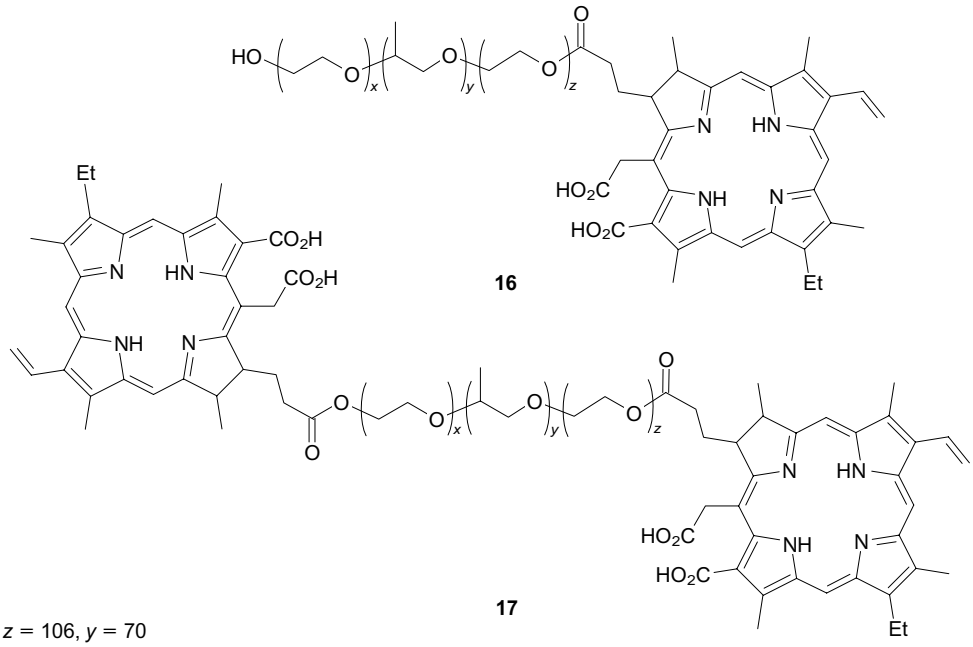
Vargas *et al.*[154] prepared mTHPP-loaded PLGA nanoparticles of three different sizes (117, 285 and 593 nm) *via* an emulsification–diffusion technique. Nanoparticles with a size of 117 nm exhibited the maximum phototoxic effect and high quantum yield for *in vitro* singlet oxygen generation due to increased intracellular uptake. This nanoparticle size proved to be more suitable for PDT.

The emulsification–diffusion approach was used to prepare different nanoparticles based on three polymers, PLA, PLGA and Eudragit, for pTHPP delivery to EGI-1 and TFK-1 cholangiocellular carcinoma cells.[155] The particle size was varied depending on the nature of the polymer from 200 to 300 nm. The efficiency of PS encapsulation in PLA and Eudragit was 80%; in PLGA, 70%. Eudragit and PLGA nanoparticles exhibited high *in vitro* cytotoxicity. The highest accumulation in cancer cells (more than 200-fold compared to free THPP) was observed for Eudragit nanoparticles, while PLGA nanoparticles exhibited the highest activation of caspase-3, which is known to initiate apoptosis.

Park and Na[156] synthesized two Chl-e_6–Pluronic F127 conjugates (compounds **16** and **17**) by the carbodiimide method. Conjugate **16**, unlike dimer **17**, has good solubility in water. The cellular internalization and phototoxicity of compound **16** were compared with the corresponding characteristics of free Chl-e_6 in CT-26 mouse cancer cells. Conjugate **16** exhibited increased cellular uptake and internalization compared to free PS. Phototoxicity of this compound was evaluated both using irradiation and in the absence of illumination. In the latter case, conjugate **16**, like Chl-e_6, did not cause cell destruction, whereas the phototoxicity of this conjugate after irradiation was three times higher compared to that of Chl-e_6. The tumour volume was reduced by 75% in the case of compound **16**; for free PS, the decrease in the tumour volume was only 43%. After the intravenous administration, conjugate **16** strongly suppressed CT-26 xenograft tumour growth.

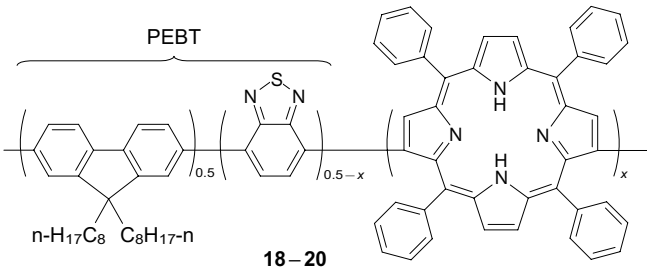
Chang *et al.*[157] synthesized polymer dots (Pdots) by the Suzuki coupling reaction using TPP, fluorene and benzothiazole as monomers. It is know that hydrophobic polymers form small stable densely packed nanoparticles. The first step involved the synthesis of the dibrominated deriv-

Structures 16, 17



16, **17**: $x = z = 106$, $y = 70$

Structures 18–20



18–20

x = 0.02 (**18**), 0.05 (**19**), 0.10 (**20**)

ative of TPP followed by the palladium-catalyzed cross-coupling of this derivative with 4,7-dibromobenzo[*c*]-1,2,3-thiadiazole and 9,9-dioctylfluorene-2,7-diboronic acid ester. Then a series of poly[(9,9-dioctylfluorene-2,7-diyl)-*alt*-*co*-(1,4-benzo-2,1,3-thiadiazole)] (PEBT) conjugates, compounds **18**–**20** with a molar fraction of TPP equal to 2%, 5% and 10%, respectively, was synthesized. The covalent attachement of porphyrin to the polymer backbone brings the polymer in close contact with the porphyrin macrocycle, thereby facilitatating the energy transfer to the TPP molecule and preventing the leaching of PS from the polymer. These polymer dots have a negative surface potential and possess a spherical morphology. The PS incorporation does not affect the particle size and morphology (Fig. 11). The covalent attachment of PS leads to fluorescence quenching of the polymer (λ_{em} = 550 nm) and, correspondingly, to a decrease in the fluorescence quantum yield. Nevertheless, the emission of TPP is sufficient for fluorescence cellular or *in vivo* imaging. The polymer dots have high quantum yields for singlet oxygen generation and good photostability. The cytotoxicity of Pdots was evaluated in MCF-7 cancer cells by the MTT assay [3-(4,5-dimethylthiazol-2-yl)-2,5-diphenyltetrazolium bromide]. At a concentration of compound **19** equal to 16 μg ml^{-1}, MCF-7 cells were completely destroyed using a light dose of 120 J cm^{-2}. The *in vivo* therapeutic efficacy of compound **19** was evaluated in tumour-bearing nude mice. The polymer dots (4 mg per kg of body weight) were injected into the tumour and then the tumour was irradiated on the first and seventh day at a power density of 100 mW cm^{-2}. The tumour growth was

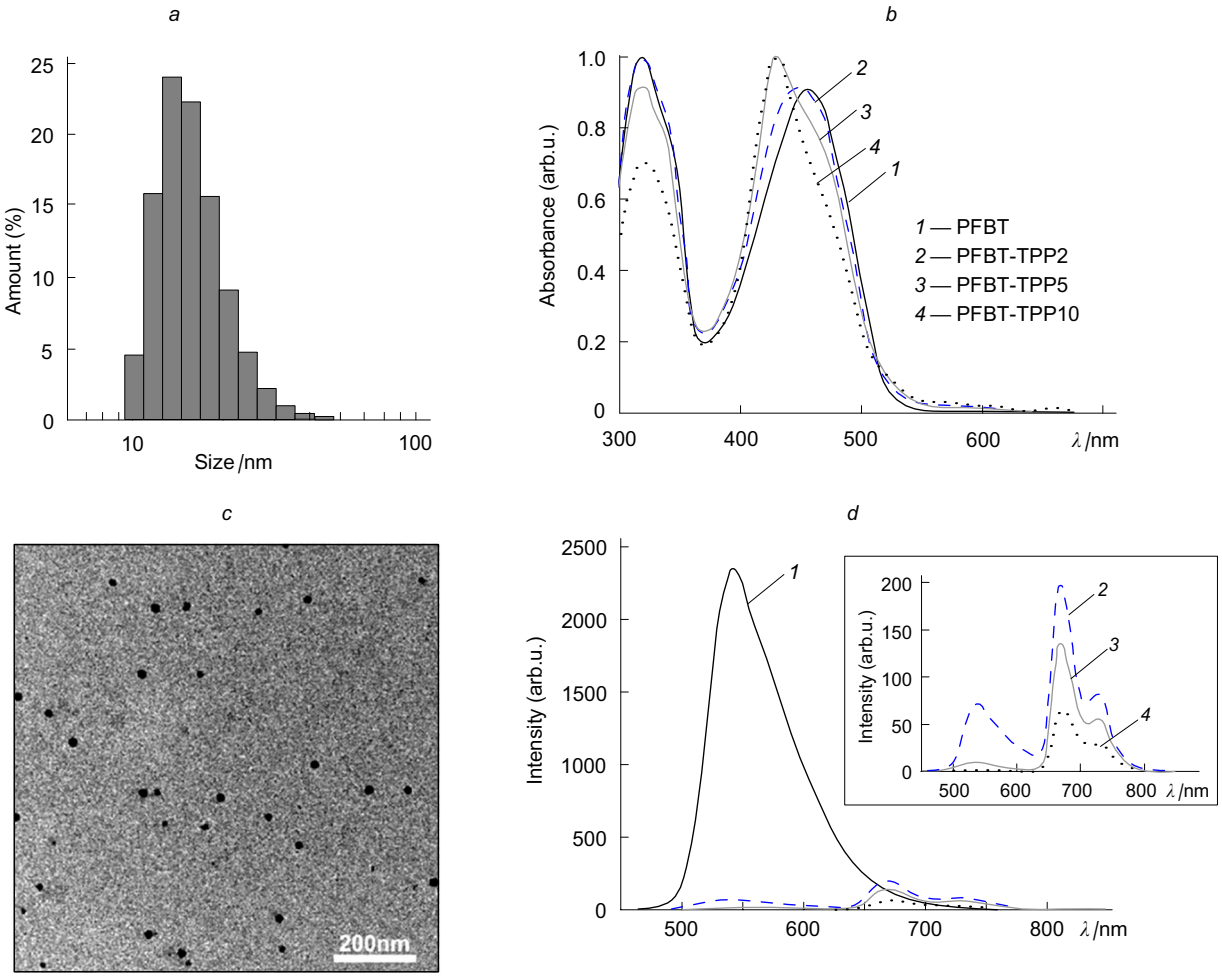


Figure 11. Size distribution of polymer dots in aqueous solution measured by dynamic light scattering (*a*), absorption spectra of PFBT polymer dots in aqueous solution (*b*), SEM images of PFBT-TPP5 polymer dots and (*c*) fluorescence spectra of PFBT and PFBT-TPP*n* polymer dots, where n = 2 (**18**), 5 (**19**) and 10 (**20**), in aqueous solution (*d*).[157]

significantly inhibited after PDT. No pathological changes were observed in the spleen, kidney, lung or heart.

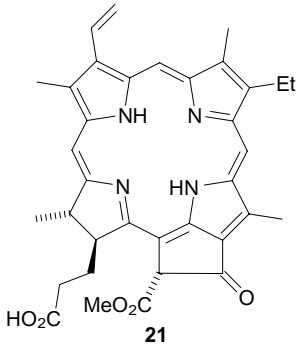
The preparation of PNPs based on polyglycolide, polylactide and poly(L,D-lactide-co-glycolide) copolymer (PLGA) was reported.[158] Copolymer-based nanoparticles were used for the encapsulation of 5-aminolevulinic acid utilized in dermatology;[159] PEGylated PLGA was employed as a delivery vehicle of different PSs for PDT of cancer.[160, 161]

Layer-by-layer PNPs were proposed for combined chemotherapy and phototherapy of cancer. These PNPs are fabricated by means of layer-by-layer assembly of positively and negatively charged polymers loaded with drugs having different solubility.[162] An example of such PNPs is a delivery system containing the PLGA core coated with lipophilic taxane Docetaxel (DTX) and then with a positively charged polyethyleneimine (PEI) layer decorated with negatively charged *meso*-tetrakis(4-sufonatophenyl)porphyrin tetrasodium salt ($TPPS_4$) and hyaluronic acid.[163] In these NPs, the porphyrin $TPPS_4$ was inactivated due apparently to aggregation, but once reaching the tumour site and releasing from NPs, $TPPS_4$ induced the active generation of singlet oxygen. In *in vitro* assays, a 10-fold increase in its accumulation was observed compared to free $TPPS_4$. The combined chemotherapy and photodynamic therapy not only substantially enhanced the chemotherapeutic effect on the tumour but also (what is the most important!) led to a 20-fold enhancement of the photodynamic effect.

Konan-Kouakou *et al.*[164] employed PLGA-based nanoparticles as a delivery vehicle for Verteporfin. Compared to free PS, PS-loaded PLGA nanoparticles were more efficient in mice with rhabdomyosarcoma M1 tumour. Thus, the mice were photosensitive at early irradiation times for only a short period. The tumour completely disappeared within 14 days after PDT. The tumour regrowth was observed in 34% mice on the 20th day.

One key point of efficiency of nanoplatforms is the mechanism of PS delivery to the cells. Kerdous *et al.*[165] studied the mechanisms of delivery of hydrophobic PS — pheophorbide *a* (**21**) — using poly(ethylene oxide)-poly(ε-caprolactone) [PEO(5000)–PCL(4000)] copolymer nanoparticles to MCF-7 cancer cells. It was shown that pheophorbide is delivered to the cells *via* two routes. The reaction rate *via* one route is high. This pathway involves the collision between the nanoparticle shell and the cell membrane, *i.e.*, pheophorbide penetrates into the cells in the non-encapsulated form. The reaction rate *via* another route is low. This pathway may be associated with cellular internalization of nanoparticles.

Structure 21



21

Boix-Garriga *et al.*[166] demonstrated the role of the chemical structure of PS in the photophysical and photochemical properties of the final nanoparticle suspension. They found that hydrophobic Zn TPP entrapped in PLGA nanoparticles does not exhibit sufficient photoactivity because the generated $^1O_2$ remains confined inside NPs. Assuming that hydrophilic PSs covalently attached to the NP surface will enhance the efficiency of singlet oxygen delivery required for cancer cell destruction, the authors prepared new formulations with the hydrophilic Zn complex of 5-(4-azidophenyl)-10,15,20-tris(*N*-methyl-4-pyridyl)porphyrin trichloride. Hydrophilic porphyrin was shown to be located at the outer surface of NPs mainly in the monomeric form. The phototoxicity of PLGA nanoparticles loaded with cationic porphyrin was higher than that of nanoparticles modified with hydrophobic porphyrin.

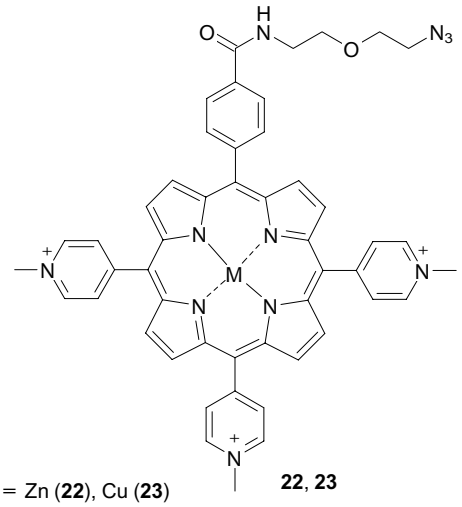
Jeong *et al.*[167] devised a biocompatible nanodispersed formulation composed of pyropheophorbide *a*, polycaprolactone (PCL) and Pluronic F-68 (clinically approved polymeric surfactant). Nanoparticles with a size of 20 nm were prepared by the microemulsification–evaporation method. The hydrophobic part of nanoparticles consisted of the PLC matrix containing well-dispersed pyropheophorbide *a* molecules. The surface was stabilized by Pluronic. These nanoparticles exhibited *in vitro* phototoxicity against HeLa cancer cells and showed efficient tumour accumulation in mice bearing skin squamous cell carcinoma, as well as significant tumour suppression. The study demonstrated great potential of these NPs as a biocompatible photosensitizing agent for PDT treatment of cancer.

Park *et al.*[168] prepared hyaluronic acid (HA)-coated PLGA nanoparticles for targeted PDT and molecular imaging. Chlorin e_6 was encapsulated into nanoparticles, which are highly tropic for the cluster of differentiation 44 (CD44) receptor. Numerous carboxylate groups of HA enabled the chelation of gadolinium ions (Gd^{3+}), which are employed as MRI contrast agents. Using *in vitro* and *in vivo* fluorescence and MRI signal analysis, the authors demonstrated that these nanoparticles bind with high affinity to CD44 receptors, which are overexpressed in A549 cancer cells. After laser irradiation in the near-IR region (NIR), a significant delay in tumour growth and tumour regression was observed. This system can be utilized as a therapeutic platform for bimodal (MR–NIR) imaging of PDT of cancer.

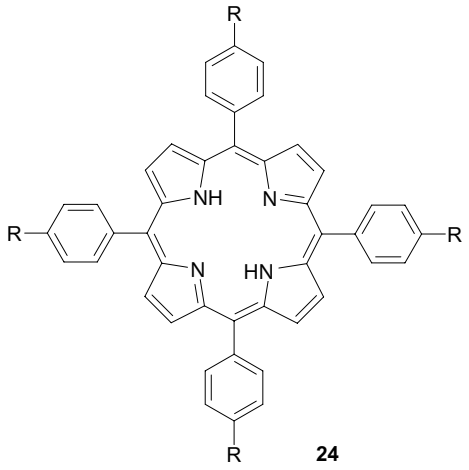
Lavado *et al.*[169] evaluated the ability of nanoparticles to generate controlled amounts of ROSs in mesenchymal stem cells. The authors synthesized polyacrylamide (PAA) nanoparticles covalently functionalized with Zn and Cu porphyrin complexes **22** and **23**. Copper porphyrin complexes were used as the control. Nanoparticles functionalized with 5%, 10% and 20% compounds **22** and **23** were prepared, with a diameter of 80 nm and a positive surface charge, to facilitate subcellular localization (zeta potential higher than +15 mV).

The controlled ROS generation was demonstrated in two series of experiments: 1) irradiation of internalized nanoparticles containing different percentage of PS with a single dose of excitation light; 2) irradiation of internalized nanoparticles functionalized with 5% compound **22** with repeated doses of excitation light. It was shown that the level of ROSs can be modulated to a desired value through the control of either the PS concentration or the light dose. Thus, nanoparticles functionalized with 5% complex **22**

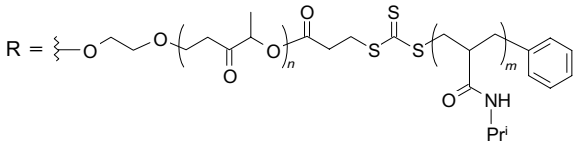
Structures 22 – 24



M = Zn (**22**), Cu (**23**) **22**, **23**



24



exhibited a considerable increase in cytotoxicity after 12 irradiations. The irradiation of nanoparticles functionalized with 5%, 10%, 15% and 20% PS led to an increase in the percentage of apoptotic cell death by 29%, 30%, 37% and 44%, respectively.

Polyionic micelles are effective in PDT of age-related macular degeneration and different kinds of neovascularization in tumours. Besides, these micelles are characterized by low accumulation in the skin, preventing undesired phototoxicity. Along with the targeted delivery, nanotechnology-based approaches allow the selective excitation of PSs in the tumour site. This is achieved through the formation of micellar structures by a glycol chitosan backbone grafted with 3-diethylaminopropyl isocyanate, chlorin e_6 and polyethylene glycol at pH 7.4. In this structure, hydrophilic PEG chains form the outer corona, while 3-diethylaminopropyl isocyanate and Chl-e_6 form the hydrophobic inner core, in which closely spaced Chl-e_6 molecules are unable to generate reactive oxygen species. However, a decreases in pH to 6.8 leads to protonation of 3-diethylaminopropyl isocyanate moieties, therewith making them hydrophilic. This leads to unfolding of the main polymer, after which PS molecules can again produce singlet oxygen under illumination. Since the extracellular fluid in the tumour is generally more acidic (pH 6.8 – 7.0) compared to the normal tissue (pH 7.4), chlorin e_6 attached to the polymer can generate reactive oxygen species only at damaged sites. Recently, Korean researchers [170, 171] demonstrated that this system is effective in nude mice already at a Chl-e_6 concentration of 0.1 mg per kg of body weight.

Thermosensitive star-shaped porphyrin-cored poly(L-lactide)-block-poly(*N*-isopropylacrylamide) (PLA – PNIPAM) was synthesized by Dai *et al.*[172] Due to the unique structure and amphiphilicity, this polymer can self-assemble in aqueous medium to form micelles with a size of 110 nm. It should be noted that the critical solution temperature and the morphology of the copolymer nanoparticles can be controlled by changing the ratio of hydrophilic PNIPAM blocks to hydrophobic PLA blocks. With decreasing PNIPAM block length, the structure of copolymer **24** in aqueous solution is transformed from spherical to wormlike micelles, and the lower critical solution temperatures of the copolymers are close to the nominal physiological temperature of 37.2 °C: 37.9, 37.2 and 35.9 °C for the $n:m$ ratios of 33 : 67, 45 : 55 and 88 : 12. The *in vitro* study showed that the polymer exhibited no significant dark cytotoxicity at concentrations up to 128 μg ml^{-1}, while being phototoxic to human BEL-7402 hepatocellular carcinoma cells.

4.3.1. Natural polymeric nanoparticles based on hyaluronic acid

Hyaluronic acid is the major component of the extracellular matrix. It is widely used for drug delivery due to biocompatibility, biodegradability, nontoxicity and non-immunogenicity; besides, HA receptors are overexpressed in many cancer cells.[173] Since HA-based nanoparticles are rapidly captured by the RES, the surface modification with polyethylene glycol is the most promising approach to increasing the circulation of these NPs. When used in a drug delivery system, hyaluronic acid can act simultaneously as a carrier and a targeting agent. However, the hydrophilic nature of HA hinders its attachment to hydrophobic PSs. Several methods were developed in order to solve this issue. Misra *et al.*[174] reported the delivery of Chl-e_6 by HA-based nanoparticles for the simultaneous photodynamic imaging and therapy. For this purpose, aminated 5-β-cholanic acid, PEG and the dye BHQ3 were chemically conjugated to HA polymers. Then Chl-e_6 was loaded into nanoparticles by dialysis. The loading efficiency of Chl-e_6 was higher than 80%. The resulting nanoparticles were stable under aqueous conditions and showed rapid uptake into tumour cells. After internalization, nanoparticles were rapidly degraded by hyaluronidase overexpressed in tumour cells, thereby releasing PS in the tumour tissue. After the intravenous injection, nanoparticles effectively accumulated in the tumour tissue *via* the passive targeting mechanism and receptor-mediated endocytosis. In the subsequent work, smart NPs were prepared based on covalent conjugates of Chl-e_6 and HA coupled *via* adipic dihydrazide (ADH).[175] The resulting nanoparticles formed stable spherical nanostructures in aqueous medium with uniform size distribution. It was shown that NPs actively disassembled in the presence of hyaluronidase, as evidenced by a fluorescence signal. Nanoparticles were rapidly taken up to human A549

lung cancer cells *via* CD44 receptors. Under laser irradiation, NPs enabled good near-infrared fluorescence and photoacoustic imaging of tumour tissues. A five-fold increase in the fluorescence intensity and a three-fold increase in the photoacoustic intensity compared to free Chl-e_6 were observed. In addition, even at low irradiation doses, NPs exhibited more effective PDT in the suppression of tumour growth compared to free Chl-e_6 in both *in vitro* and *in vivo* assays. In general, the results indicate that these NPs are promising biocompatible nanoplatforms for simultaneous dual-modal tumour imaging and phototherapy.

Li *et al.*[176] fabricated self-assembled nanogels (particle size was ~200 nm) based on covalent conjugate **25**, acetylated HA and pheophorbide *a*. The distinguishing feature of these nanogels is self-quenching in phosphate buffer. Their fluorescence intensity strongly depends on the amount of pheophorbide *a* in an organic solvent (DMSO or DMF) and decreases with increasing PS concentration. After incubation with HeLa cells, the degradation of HA nanoparticles by intracellular enzymes in endosomes and lysosomes led to fluorescence recovery. Studies by confocal spectroscopy and FACS analysis (fluorescence-activated cell sorting), which is a specialized type of flow cytometry, showed that nanogels are rapidly internalized into HeLa cells *via* an HA-induced endocytosis mechanism. These results indicate that HA-based nanogels can potentially be applied in photodynamic therapy. Han *et al.*[177] developed new nanoparticles for the combined PD and PT therapy. The nanoparticle core consisted of biodegradable and biocompatible polydopamine, which was prepared from a synthetic eumelanin polymer coated with a pheophorbide–HA conjugate synthesized earlier. Nanoparticles were actively internalized *via* receptor-mediated endocytosis involving lymphatic vessel endothelial receptor 1 (LYVE-1) of clusters of differentiation 44 and 168 (CD44, CD168) (Fig. 12). The nanoparticle shell in the tumour cell environment rapidly degraded to release PS and dopamine nanoparticles. Chlorin e_6 efficiently generated ROS, and the dopamine moiety was involved in photothermal therapy.

The self-assembly of hydrophilic biomolecules is hindered. Sun *et al.*[178] proposed a strategy to fabricate stable hyaluronic acid nanoparticles without the need of modifying with hydrophobic groups.[178] This approach involves the electrostatic assembly of hyaluronic acid and naturally produced ε-polylysine followed by the *in situ* cross-linking

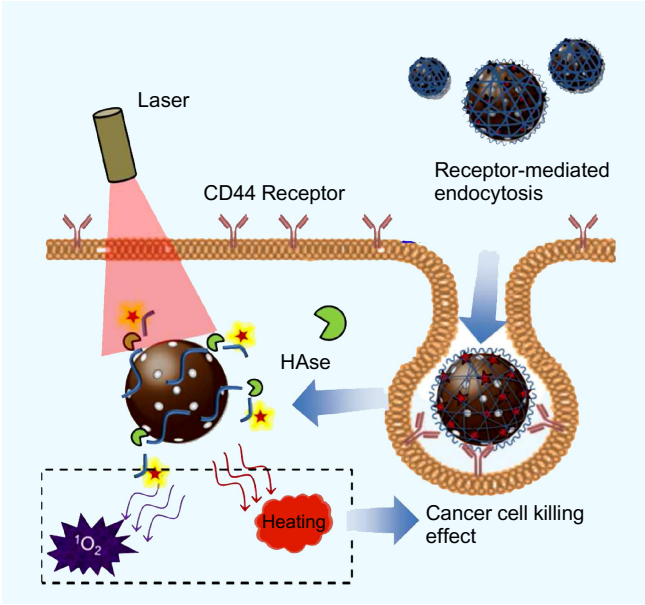


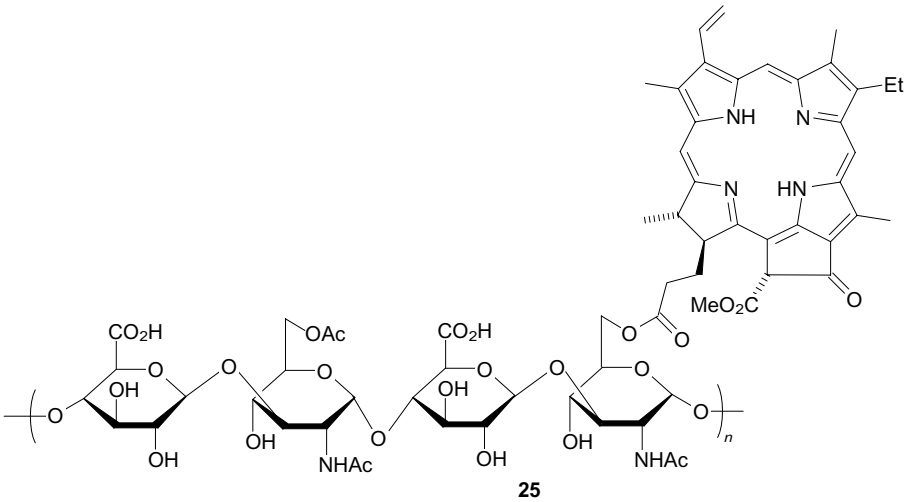
Figure 12. Mechanism of nanoparticle internalization *via* receptor-mediated endocytosis (HAse is hyaluronidase).[177]

by disulfide bonds and the encapsulation of Chl-e_6 in the resulting nanoparticles. Chlorin Chl-e_6 can be released in response to changes in pH and concentration of glutathione-SH (GSH). It was found that Chl-e_6-loaded nanoparticles displayed enhanced *in vitro* cellular uptake by MCF-7 cancer cells, improved phototoxicity and better biocompatibility compared to free PS.

4.3.2. Natural polymeric nanoparticles based on chitosan

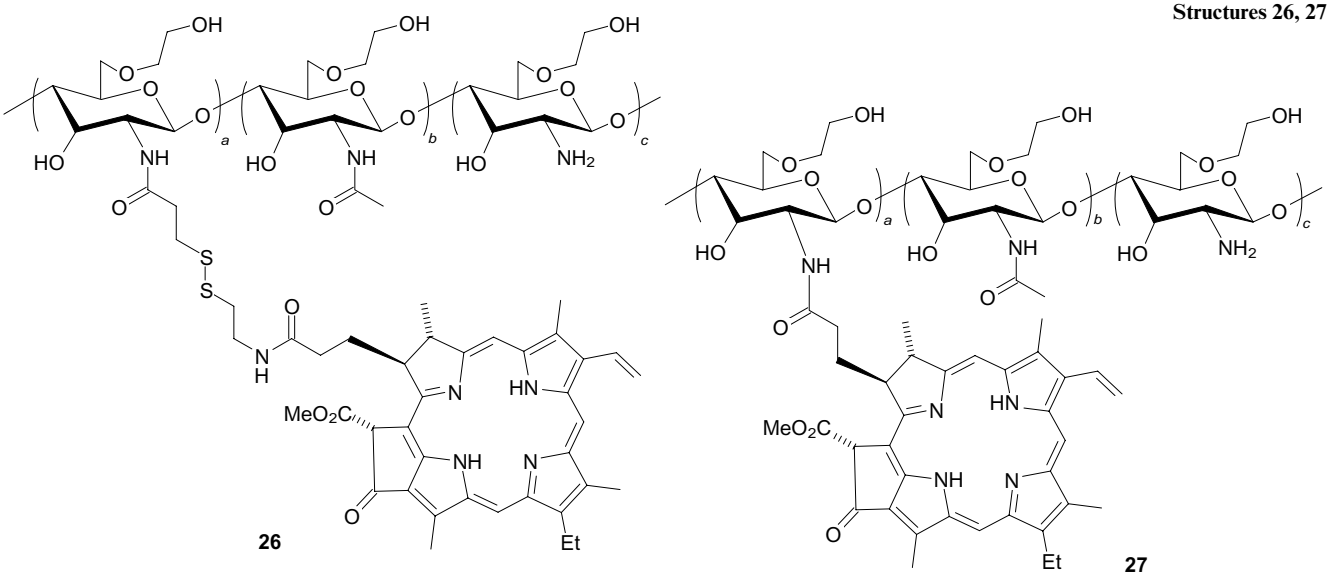
Chitosan is a natural linear polysaccharide composed of β-(1-4)-D-glucosamine and *N*-acetyl-D-glucosamine. It is a deacetylated derivative of chitin, which is the second most abundant biopolymer after cellulose. Chitosan has biocompatibility, biodegradability and low immunogenicity due to which it is widely used in biomedicine.[179,180] Besides, chitosan is known to enhance mucosal drug delivery without damaging tissues. Chitosan is insoluble in water and organic solvents but can be dissolved in acidic medium. To prepare nanoparticles, chitosan is modified with hydro-

Structure 25



25

Structures 26, 27



phobic groups, *e.g.*, bile or fatty acids.[181] Chitosan derivatives conjugated to a hydrophobic moiety self-assemble into nanoparticles in aqueous medium.[182]

Lee *et al.*[183] synthesized chitosan nanoparticles modified with ethylene glycol for protoporphyrin IX delivery. In *in vivo* experiments, the uptake of these nanoparticles by squamous cell carcinoma (SCC7) cells in nude mice was 2.3 times higher than in other organs. Moreover, the fluorescent total photon counts per organ from tumour tissues were 1.49 to 3.8 times higher compared to other organs, which is indicative of the predominant nanoparticle uptake by the tumour. On the 14th day after the treatment with these NPs, the tumour volume reduced by 44% compared to mice treated with free Proto IX. Besides, the histological examination showed that most tumour cells in mice treated with nanoparticles were severely damaged or destroyed, while residual tumour was present in mice that received free Proto IX. Noncolvalent PS loading of nanoparticles can lead to uncontrolled PS release. To tackle this issue, the same research group[184] developed a chemical modification of chitosan in order to prepare new Proto IX-based nanoparticles. The authors showed that these particles are released in a controlled manner in tumour cells, while being inactive (quenched) in the bloodstream. Therefore, the cellular uptake of chemically modified chitosan in HT-29 human colon adenocarcinoma tumour-bearing mice was 1.4- and 2.1-fold higher than that of nanoparticles noncovalently loaded with Proto IX and of free protoporphyrin, respectively. The authors observed a five-fold tumour volume reduction in mice treated with chitosan-conjugated PS and severe cell death in tumour tissues.

In another study,[185] chitosan was modified with hydrophobic ursodeoxycholic acid (UDCA) in order to deliver Chl-e_6 to HuCC-T1 cholangiocarcinoma cells. Chlorin e_6 was incorporated into nanoparticles through the formation of ionic complexes. The size of the resulting spherical NPs was 200–400 nm. The results of PDT experiments showed that chitosan nanoparticles enhanced Chl-e_6 uptake into tumour cells, increased ROS generation and improved phototoxicity compared to free Chl-e_6.

Oh *et al.*[186] synthesized two types of glycol chitosan nanoparticles modified with pheophorbide *a* through disulfide (**26**) and amide (**26**, **27**) bonds. These amphiphilic conjugates self-assembled in aqueous media to form stable nanoparticles, retaining switchable photoactivity. In aqueous medium, photoactivity was strongly suppressed by their self-quenching effect, and nanoparticles were inactive. After uptake by cancer cells, disulfide bonds in nanoparticles **26** were cleaved, resulting in PS release. As opposed to compound **27**, nanoparticles **26** rapidly recovered their photoactivity. Besides, conjugate **26** exhibited prolonged blood circulation, thereby enhancing its accumulation in cancer cells. Nanoparticles **26** showed good *in vivo* therapeutic efficacy in mice bearing HT-29 tumour (humanized colon cancer cells).

Chen and co-workers[187] proposed vitamin-E-grafted chitosan nanoparticles as a delivery vehicle for Temoporfin. The nanoparticles were additionally decorated with cyclic RGD peptide capable of specific interaction with $\alpha_v\beta_3$-integrin receptor-rich tumours (Fig. 13). Spherical RGD NPs

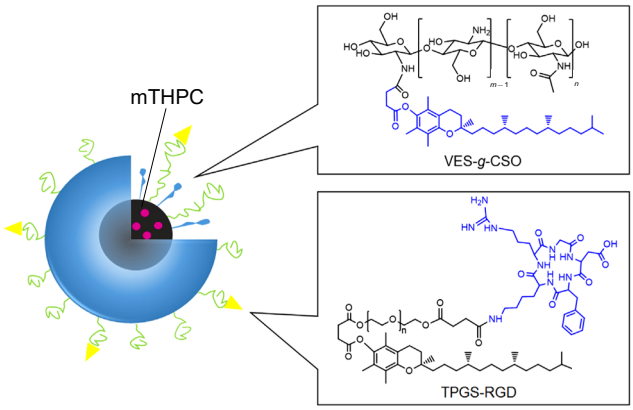


Figure 13. Schematic illustration of nanoparticles prepared in Ref. 187.
mTHPC is temoporfin; VES-g-CSO is vitamin E succinate-grafted chitosan; TPGS-RGD is D-α-tocopheryl polyethylene glycol succinate–cyclic peptide conjugate.

with a size of 145 nm were internalized by $\alpha_v\beta_3$-integrin receptors in U87MG glioblastoma cells. After irradiation, RGD NPs effectively generate singlet oxygen. Nanoparticles modified with RGD peptide showed higher antitumour efficacy and lower systemic toxicity compared to unmodified nanoparticles in subcutaneous tumour-bearing nude mice.

5. Conclusion

Photodynamic therapy is an effective non-invasive treatment modality for cancer. However, because of certain limitations associated primarily with the utilized PSs, its potential is not fully realized. First- and second-generation photosensitizers can eliminate superficial and not-deep-seated tumours, but are ineffective against pigmented neoplasms. Besides, the utilization of hydrophobic PSs capable of penetrating into cancer cells is greatly limited by poor solubility of these compounds in water and their aggregation, leading to a significant decrease in the quantum yields of fluorescence and singlet oxygen generation. Third-generation photosensitizers that have light absorption in the near-IR region will greatly increase the potential of PDT. Bacteriochlorophyll-based PSs are highly promising in this respect, because they possess intense absorption at 800 nm, where the depth of light penetration into tissues is 20 mm. However, high hydrophobicity of these compounds is a serious obstacle for the development of such PSs. New efficient drug delivery systems are required for the successful application of these PSs.

This area of research offers considerable promise in PDT of cancer. Thus, different delivery systems are being developed for passive and active targeting of tumour cells. The surface functionalization of the cells with targeting ligands is a promising approach because it allows a significant increase in the selectivity of nanoparticle accumulation in cancer cells. Advances in molecular biology enabling the selection of ligands and deeper insight into molecular mechanisms of the disease and mechanisms of drug releases are important for understanding the mechanisms of targeted delivery. The development of endogenous and exogenous stimuli-responsive nanoparticles is another rapidly growing area of research. The use of such nanoparticles increases the accumulation of PSs in the tumour and diminishes light responsivity of normal tissues.

The absence of clinical trials for a considerable number of available nanoparticles is related to the difficulties in applying them in practice. In particular, this is associated with the scaling up of *in vitro* and *in vivo* assays [188] and the necessity of preparing pure and uniform nanoparticles, obtaining precise and reproducible results and establishing standardized protocols for safety and validation. We believe that the success in this field can be achieved in close cooperation between chemists, biochemists and physicians.

A.F.Mironov is grateful to the Russian Science Foundation (Project No. 16-13-10092) for the financial support for the preparation of the Section devoted to lipid nanoparticles. K.A.Zhdanova thanks the Russian Science Foundation (Project No. 17-73-10470) for the financial support for the preparation of the Section devoted to polymeric nanoparticles.

Figures 2 and 4 are courtesy of the Royal Society of Chemistry; Figures 5, 7, 9, 11 and 12 are courtesy of the American Chemical Society; Figures 8 and 13 are courtesy of Elsevier; Figure 10 is courtesy of John Wiley and Sons.

References

1. T.J.Dougherty, C.J.Gomer, B.W.Henderson, G.Jori, D.Kessel, M.Korbelik, J.Moan, Q.J.Peng. *Nat. Cancer Inst.*, **90**, 889 (1998)
2. R.Bonnett. *Chemical Aspects of Photodynamic Therapy*. (Amsterdam: Gordon and Breach Sci. Publ., 2000)
3. A.F.Mironov. *Sovremennye Problemy Lazernoi Fiziki. (Itogi Nauki i Tekhniki)*. [Current Problems of Laser Physics. (Advances in Science and Engineering)]. (Moscow: Izd. VINITI, 1990). Vol. 3. P. 5
4. E.F.Stranadko, V.N.Kamenskaya. *Laser. Med.,* **17** (2), 44 (2013)
5. E.A.Sheiko, V.A.Sustretov, A.I.Shihlyarova. *Int. J. Appl. Fundam. Res.*, **10**, 658 (2015)
6. N.F.Gamaleia, I.O.Shton. *Photodiagn. Photodyn. Ther.*, **12**, 221 (2015)
7. G.Kandasamy, D.Maity. *Int. J. Pharm.*, **496**, 191 (2015)
8. O.Penon, M.J.Marín, D.B.Amabilino, D.A.Russell, L.Pérez-García. *J. Colloid Interface Sci.*, **462**, 154 (2016)
9. C.Frochot, A.Sève, R.Vanderesse, M.Toussaint, M.Barberi-Heyob, in *Applications of Nanoscience in Photomedicine. (Ser. Woodhead Publishing Series in Biomedicine)*. (Eds M.R.Hamblin, P.Avci). (Amsterdam: Elsevier, 2015). P. 449
10. I.Marangon, C.Ménard-Moyon, A.K.A.Silva, A.Bianco, N.Luciani, F.Gazeau. *Carbon*, **97**, 110 (2016)
11. E.A.Grebenik, A.B.Kostyuk, S.M.Deyev. *Russ. Chem. Rev.*, **85**, 1277 (2016)
12. A.N.Generalova, I.K.Kochneva, E.V.Khaydukov, V.A.Semchishen, A.E.Guller, A.V.Nechaev, A.B.Shekhter, V.P.Zubov, A.V.Zvyagin, S.M.Deyev. *Nanoscale*, **7**, 1709 (2015)
13. D.Hu, L.Chen, Y.Qu, J.Peng, B.Chu, K.Shi, Y.Hao, L.Zhong, M.Wang, Z.Qian. *Theranostics*, **8**, 1558 (2018)
14. E.O.Serebrovskaya, E.F.Edelweiss, O.A.Stremovskiy, K.A.Lukyanov, D.M.Chudakov, S.M.Deyev. *Proc. Natl. Acad. Sci. USA*, **106**, 9221 (2009)
15. K.E.Mironova, G.M.Proshkina, A.V.Ryabova, O.A.Stremovskiy, S.A.Lukyanov, R.V.Petrov, S.M.Deyev. *Theranostics*, **3**, 831 (2013)
16. A.F.Mironov. *Uspekhi Khimii Porfirinov*. (Progress in Porphyrin Chemistry). (Ed. O.A.Golubchikov). (St. Petersburg: Institute of Chemistry SPbU, 1997). Vol. 1. P. 357
17. M.Ethirajan, Y.Chen, P.Joshi, R.K.Pandey. *Chem. Soc. Rev.*, **40**, 340 (2011)
18. L.Polo, G.Valduga, G.Jori, E.Reddi. *Int. Biochem. Cell Biol.*, **34**, 10 (2002)
19. N.Gueddari, G.Favre, H.Hachem, E.Marek, F.Le Gaillard, G.Soula. *Biochimie*, **75**, 811 (1993)
20. F.Yuan, M.Leuning, D.A.Berk, R.K.Jain. *Microvasc. Res.*, **45**, 269 (1993)
21. N.A.Bragina, K.A.Zhdanova, A.F.Mironov. *Russ. Chem. Rev.*, **85**, 477 (2016)
22. H.Abrahamse, M.R.Hamblin. *Biochem J.*, **473**, 347 (2016)
23. P.Mroz, J.T.Hashmi, Y.Y.Huang, N.Lange, M.R.Hamblin. *Exp. Rev. Clin. Immunol.*, **7**, 75 (2011)
24. Y.Miri, J.Akioto, K.Moritare, C.Hironaka, Y.Fujiwara. *Laser Med. Sci.*, **30**, 1739 (2015)
25. H.Vakifahmetoglu-Norbeerg, A.T.Ouchida, E.Norberg. *Biochem. Biophys. Res. Commun.*, **482**, 426 (2017)
26. E.Buytaert, M.Dewaele, P.Agostinis. *Biochim. Biophys. Acta*, **1776**, 86 (2007)

27. H.Maes, N.Rubio, A.D.Garg, P.Agostinis. *Trends Mol. Med.*, **19**, 428 (2013)
28. A.D.Garg, H.Maes, E.Romano, P.Agostinis. *Photochem. Photobiol. Sci.*, **14**, 1410 (2015)
29. F.Moret, E.Reddi. *J. Porphyrins Phthalocyanines*, **21**, 239 (2017)
30. A.B.Ormond, H.S.Freeman. *Materials*, **6**, 817 (2013)
31. J.M.Dabrowski, L.G.Arnaut. *Photochem. Photobiol. Sci.*, **14**, 1765 (2015)
32. M.A.Grin, A.F.Mironov. *Russ. Chem. Bull., Int. Ed.*, **65**, 333 (2016)
33. I.V.Pantyushenko, M.A.Grin, R.I.Yakubovskaya, E.A.Plotnikova, N.B.Morozova, A.A.Tsyganov, A.F.Mironov. *Vestn. MITKHT*, **9**, 3 (2014)
34. M.A.Biel. *Laryngoscope*, **108**, 1259 (1998)
35. J.Feyh. *J. Photochem. Photobiol., B*, **36**, 175 (1996)
36. L.Zang, H.Zhao, Q.Fang, M.Fan, T.Chen, Y.Tian, J.Yao, Y.Zheng, Z.Zhang, W.Cao. *J. Porphyrins Phthalocyanines*, **21**, 59 (2017)
37. A.F.Mironov. *Russ. Chem. Rev.*, **82**, 333 (2013)
38. S.S.Lucky, K.C.Soo, Y.Zhang. *Chem. Rev.*, **115**, 1990 (2015)
39. A.Scherz, Y.Salomon, J.Coleman. *Photodiagn. Photodyn. Ther.*, **17**, 22(2017)
40. T.A.Debele, S.Peng, H.-C.Tsai. *Int. J. Mol. Sci.*, **16**, 22094 (2015)
41. A.Bugaj. *Photochem. Photobiol. Sci.*, **10**, 1097 (2011)
42. Y.N.Konan, R.Gurny, E.Allemann. *J. Photochem. Photobiol., B*, **66**, 89 (2002)
43. M.Shakiba, J.Chen, G.Zheng. *Appl. Nanosci. Photomed.*, **24**, 511 (2015)
44. Y.Ang, S.Y.Tan, Y.Zhao. *Org. Biomol. Chem.*, **12**, 4776 (2014)
45. T.L.Andresen, D.H.Thompson, T.Kaasgaard. *Mol. Membr. Biol.*, **27**, 353 (2010)
46. N.V.Rukosueva, D.A.Bezrukov, A.P.Kaplun, V.I.Shvets. *Vopr. Biol., Med. Farm. Khim.*, **12** (10), 3 (2014)
47. M.V.Leonova, Yu.B.Belousov. *Klin. Farmokol. Terap.*, **18** (2), 62 (2009)
48. A.S.L.Derycke, P.A.M.de Witte. *Adv. Drug Deliv. Rev.*, **56**, 17 (2004)
49. R.Weijer, M.Broekgaarden, M.Kos, R.van Vught, E.A.J.Rauws, E.Breukink, T.M.van Gulik, G.Storm, M.Heger. *J. Photochem. Photobiol., C*, **23**, 103 (2015)
50. D.D.Lasic, F.J.Martin, A.Gabizon, S.K.Huang, D.Papahadjopoulos. *Biochim. Biophys. Acta*, **1070**, 187 (1991)
51. V.P.Torchilin. *Drug Discov.*, **4**, 145 (2005)
52. A.S.Ulrich. *Biosci. Rep.*, **22**, 129 (2002)
53. K.Nawalany, A.Rusin, M.Kepczynski, A.Mikhailov, G.Kramer-Marek, M.Snietura, J.Poltowicz, Z.Krawczyk, M.Nowakowska. *J. Photochem. Photobiol., B*, **97**, 8 (2009)
54. K.Nawalany, A.Rusin, M.Kepczynski, M.Filipczak, M.Kumorek, B.Kozik, H.Weitman, B.Ehrenberg, Z.Krawczyk, M.Nowakowska. *Int. J. Pharm.*, **430**, 129 (2012)
55. A.L.Klibanov, K.Maruyama, V.P.Torchilin, L.Huang. *FEBS Lett.*, **268**, 235 (1990)
56. A.Weiss, H.van den Bergh, A.W.Griffioen, P.Nowak-Sliwinska. *Biochim. Biophys. Acta*, **1826**, 53 (2012)
57. R.K.Chowdhary, I.Shariff, D.J.Dolphin. *Pharm. Pharm. Sci.*, **6**, 13 (2003)
58. M.Varano, P.Iacono, P.Giorno, A.Chiaravalloti, M.Parravano. *Ophthalmologica*, **231**, 204 (2014)
59. P.M.R.Pereira, B.Korsak, B.Sarmento, R.J.Schneider, R.Fernandes, J.P.C.Tomé. *Org. Biomol. Chem.*, **13**, 2518 (2015)
60. A.Hogan, U.Behan, D.J.Kilmartin. *Br. J. Ophthalmol.*, **89**, 1109 (2005)
61. T.Tammela, A.Saaristo, T.Holopainen, S.Yla-Herttuala, L.C.Andersson, S.Virolainen, I.Immonen, K.Alitalo. *Sci. Transl. Med.*, **3** (69), 69ra11 (2011)
62. H.-P.Lassalle, D.Dumas, S.Grafe, M.-A.D'Hallewin, F.Guilleminand, L.Bezdetnaya. *J. Control. Release*, **134**, 118 (2009)
63. M.A.D'Hallewin, D.Kochetkov, Y.Viry-Babel, A.Leroux, E.Werkmeister, D.Dumas, S.Grafe, V.Zorin, F.Guillemin, L.Bezdetnaya. *Lasers Surg. Med.*, **40**, 543 (2008)
64. V.Reshetov, V.Zorin, A.Siupa, M.A.D'Hallewin, F.Guillemin, L.Bezdetnaya. *Photochem. Photobiol.*, **88**, 1256 (2012)
65. V.Reshetov, H.-P.Lassalle, A.Francois, D.Dumas, S.Hupont, S.Gräfe, V.Filipe, W.Jiskoot, F.Guillemin, V.Zorin, L.Bezdetnaya. *Int. J. Nanomed.*, **8**, 3817 (2013)
66. E.Gaio, D.Scheglmann, E.Reddi, F.Moret. *J. Photochem. Photobiol., B*, **161**, 244 (2016)
67. F.Jiang, L.Lilge, G.Joseph, Y.Li, M.D.Wilson, M.Chopp. *Lasers Surg. Med.*, **22**, 74 (1998)
68. F.Jiang, L.Lilge, B.Logie, Y.Li, M.Chopp. *Photochem. Photobiol.*, **65**, 701 (1997)
69. A.Igarashi, H.Konno, T.Tanaka, S.Nakamura, Y.Sadzuka, T.Hirano, Y.Fujise. *Toxicol. Lett.*, **145**, 133 (2003)
70. F.L.Primo, M.V.Bentley, A.C.Tedesco. *J. Nanosci. Nanotechnol.*, **8**, 340 (2008)
71. Y.P.Fang, P.C.Wu, Y.H.Tsai, Y.B.Huang. *J. Liposome Res.*, **18**, 31 (2008)
72. G.Shim, S.Lee, Y.B.Kim, C.W.Kim, Y.K.Oh. *Nanotechnology*, **22**, 365101 (2011)
73. A.Yuan, X.Tang, X.Qiu, K.Jiang, J.Wu, Y.Hu. *Chem. Commun.*, **51**, 3340 (2015)
74. M.Przybylo, D.Glogocka, J.W.Dobrucki, K.Fraczkowska, H.Podbielska, M.Kopaczynska, T.Borowik, M.Langner. *Eur. J. Pharm. Sci.*, **85**, 39 (2016)
75. A.Makky, J.P.Michel, A.Kasselouri, E.Briand, P.Maillard, V.Rosilio. *Langmuir*, **26**, 12761 (2010)
76. S.Ballut, D.Naud-Martin, B.Loock, P.Maillard. *J. Org. Chem.*, **76**, 2010 (2011)
77. A.Makky, J.P.Miche, P.Maillard, V.Rosilio. *Biochim. Biophys. Acta*, **1808**, 656 (2011)
78. S.Ballut, A.Makky, B.Chauvin, J.-P.Michel, A.Kasselouri, P.Maillard, V.Rosilio. *Org. Biomol. Chem.*, **10**, 4485 (2012)
79. Y.Zhou, X.Liang, Z.Dai. *Nanoscale*, **8**, 12394 (2016)
80. K.A.Carter, S.Shao, M.I.Hoopes, D.Luo, B.Ahsan, V.M.Grigoryants, W.Song, H.Huang, G.Zhang, R.K.Pandey, J.Geng, B.A.Pfeifer, C.P.Scholes, J.Ortega, M.Karttunen, J.F.Lovell. *Nat. Commun.*, **5**, 3546 (2014)
81. D.Luo, K.A.Carter, A.Razi, J.Geng, S.Shao, D.Giraldo, U.Sunar, J.Ortega, J.F.Lovell. *Biomaterials*, **75**, 193 (2016)
82. S.Shao, J.Geng, H.A.Yi, S.Gogia, S.Neelamegham, A.Jacobs, J.F.Lovell. *Nat. Chem.*, **7**, 438 (2015)
83. J.Rieffel, F.Chen, J.Kim, G.Chen, W.Shao, S.Shao, U.Chitgupi, R.Hernandez, S.A.Graves, R.J.Nickles, P.N.Prasad, C.Kim, W.Cai, J.F.Lovell. *Adv. Mater.*, **27**, 1785 (2015)
84. D.Luo, K.A.Carter, A.Razi, J.Geng, S.Shao, C.Lin, J.Ortega, J.F.Lovell. *J. Control. Release*, **220**, 484 (2015)
85. J.F.Lovell, C.S.Jin, E.Huynh, H.Jin, C.Kim, J.L.Rubinstein, W.C.Chan, W.Cao, L.V.Wang, G.Zheng. *Nat. Mater.*, **10**, 324 (2011)
86. E.Huynh, J.F.Lovell, B.L.Helfield, M.Jeon, C.Kim, D.E.Goertz, B.C.Wilson, G.Zheng. *J. Am. Chem. Soc.*, **134**, 16464 (2012)
87. C.S.Jin, J.Chen, G.Zheng, in *Proceedings of 8th International Conference on Porphyrins and Phthalocyanines (ICPP-8). Istanbul, Turkey*. 2014. P. 558
88. K.K.Ng, M.Takada, K.Harmatys, J.Chen, G.Zheng. *ACS Nano*, **10**, 4092 (2016)
89. N.Oku, T.Ishii. *Methods Enzymol.*, **465**, 313 (2009)
90. F.Moret, D.Scheglmann, E.Reddi. *Photochem. Photobiol. Sci.*, **12**, 823 (2013)

91. J.Chen, M.Jarvi, P.Lo, K.Stefflova, B.C.Wilson, G.Zheng. *Photochem. Photobiol. Sci.*, **6**, 1311 (2007)
92. A.Yavlovich, B.Smith, K.Gupta, R.Blumenthal, A.Puri. *Mol. Membr. Biol.*, **27**, 364 (2010)
93. T.L.Andresen, S.S.Jensen, K.Jorgensen. *Prog. Lipid Res.*, **44**, 68 (2005)
94. P.Majumdar, R.Nomula, J.Zhao. *J. Mater. Chem. C*, **2**, 5982 (2014)
95. M.Bikram, J.L.West. *Expert Opin. Drug Deliv.*, **5**, 1077 (2008)
96. X.Tan, X.Pang, M.Lei, M.Ma, F.Guo, J.Wang, M.Yu, F.Tan, N.Li. *Int. J. Pharm.*, **503**, 220 (2016)
97. K.Hiraka, M.Kanehisa, M.Tamai, S.Asayama, S.Nagaoka, K.Oyaizuc, M.Yuasa, H.Kawakami. *Colloids Surf., B*, **67**, 54 (2008)
98. S.Asayama, N.Kasugai, S.Nagaoka, S.Kubota, H.Kawakami. *J. Inorg. Biochem.*, **101**, 261 (2007)
99. M.Yuasa, K.Oyaizu, A.Horiuchi, A.Ogata, T.Hatsugai, A.Yamaguchi, H.Kawakami. *Mol. Pharm.*, **1**, 387 (2004)
100. G.A.M.S.van Dongen, G.W.M.Visser, M.B.Vrouenraets. *Adv. Drug Deliv. Rev.*, **56**, 31 (2004)
101. S.Oliveira, R.Heukers, J.Sornkom, R.J.Kok, P.M.P.B.Henegouwen. *J. Control. Release*, **172**, 607 (2013)
102. S.M.Deyev, E.N.Lebedenko, L.E.Petrovskaya, D.A.Dolgikh, A.G.Gabibov, M.P.Kirpichnikov. *Russ. Chem. Rev.*, **84**, 1 (2015)
103. L.C.Bergstrom, I.Vucenik, I.K.Hagen, S.A.Chernomorsky, R.D.Poretz. *J. Photochem. Photobiol., B*, **24**, 17 (1994)
104. Y.Mir, S.A.Elrington, T.Hasan. *Nanomedicine*, **9**, 1114 (2013)
105. S.Wang, G.Hüttmann, T.Hasan, R.Rahmanzadeh, in *Proceedigs Volume 9694, Optical Methods for Tumor Treatment and Detection: Mechanisms and Techniques in Photodynamic Therapy XXV. San Francisco, CA*. 2016. P. 969400; doi: 10.1117/12.2217572
106. A.Gijsens, A.Derycke, L.Missiaen, D.De Vos, J.Huwyler, P.de Witte. *Int. J. Cancer*, **101**, 78 (2002)
107. A.Roby, S.Erdogan, V.P.Torchilin. *Cancer Biol. Ther.*, **6**, 1136 (2007)
108. S.Tangutoori, B.Q.Spring, Z.Mai, A.Palanisami, L.Mensah, T.Hasan. *Nanomedicine*, **12**, 223 (2016)
109. M.García-Díaz, S.Nonell, Á.Villanueva, J.C.Stockert, M.Canete, A.Casadó, M.Mora, M.L.Sagristá. *Biochim. Biophys. Acta*, **1808**, 1063 (2011)
110. A.O.Abu-Yousif, A.C.E.Moor, X.Zheng, M.D.Savellano, W.Yu, P.K.Selbo, T.Hasan. *Cancer Lett.*, **321**, 120 (2012)
111. S.Steeland, R.E.Vandenbroucke, C.Libert. *Drug Discov. Today*, **21**, 1076 (2016)
112. A.Garud, D.Singh, N.Garud. *Int. Curr. Pharm. J.*, **11**, 384 (2012)
113. S.Kuchler, M.R.Radowski, T.Blaschke, M.Dathe, J.Plendl, R.Haag, M.Schafer-Korting, K.D.Kramer. *Eur. J. Pharm. Biopharm.*, **71**, 243 (2009)
114. F.P.Navarro, G.Creusat, C.Frochot, A.Moussaron, M.Verhille, R.Vanderesse, J.-S.Thomann, P.Boisseau, I.Texier, A.-C.Couffin, M.Barberi-Heyob. *J. Photochem. Photobiol., B*, **130**, 161 (2014)
115. S.H.Voon, L.V.Kiew, H.B.Lee, S.H.Lim, M.I.Noordin, A.Kamkaew, K.Burgess, K.L.Y.Chung. *Small*, **10**, 4993 (2014)
116. J.V.John, C.-W.Chung, R.P.Johnson, Y.-I.Jeong, K.-D.Chung, D.H.Kang, H.Suh, H.Chen, I.Kim. *Biomacromolecules*, **17**, 20 (2016)
117. G.V.Ponomarev, M.N.Solovieva, N.O.Dugin, M.G.Zavialova, A.R.Mehtiev, A.Yu.Misharin, R.A.Novikov, Ya.V.Tkachev, V.I.Popenko, V.P.Timofeev. *Bioorg. Med. Chem.*, **21**, 5420 (2013)
118. S.Tachikawa, M.E.El-Zaria, R.Inomata, S.Sato, H.Nakamura. *Bioorg. Med. Chem.*, **22**, 4745 (2014)
119. S.Tachikawa, S.Sato, H.Hazama, Y.Kaneda, K.Awazu, H.Nakamura. *Bioorg. Med. Chem.*, **23**, 7578 (2015)
120. Y.Yi, G.Lin, S.Chen, J.Liu, H.Zhang. *Mater. Sci. Eng. C*, **83**, 218 (2018)
121. K.Kataoka, A.Harada, Y.Nagasaki. *Adv. Drug Deliv. Rev.*, **47**, 113 (2001)
122. D.S.Pelosi, A.L.Tessaro, F.Moret, E.Gaio, E.Reddi, W.Caetano, F.Quaglia, N.Hioka. *J. Photochem. Photobiol., A*, **314**, 143 (2016)
123. L.Lamch, U.Bazylinska, J.Kulbacka, J.Pietkiewicz, K.Biezunska-Kusia, K.A.Wilka. *Photodiagn. Photodyn. Ther.*, **11**, 570 (2014)
124. A.Roby, S.Erdogan, V.P.Torchilin. *Eur. J. Pharm. Biopharm.*, **62**, 235 (2006)
125. H.Nakamura, L.Liao, Y.Hitaka, K.Tsukigawa, V.Subr, J.Fang, K.Ulbrich, H.Maeda. *J. Control. Release*, **165**, 191 (2013)
126. H.Koo, H.Lee, S.Lee, K.H.Min, M.S.Kim, D.S.Lee, Y.Choi, I.C.Kwon, K.Kim, S.Y.Jeong. *Chem. Commun.*, **46**, 5668 (2010)
127. D.S.Pellosi, F.Moret, A.Fraix, N.Marino, S.Maiolino, E.Gaio, N.Hioka, E.Reddi, S.Sortino. *Int. J. Nanomed.*, **11**, 4479 (2011)
128. T.Wang, D.Wang, H.Yu, M.Wang, J.Liu, B.Feng, F.Zhou, Q.Yin, Z.Zhang, Y.Huang, Y.Li. *ACS Nano*, **10**, 3496 (2016)
129. K.K.Ng, J.F.Lovell, G.Zheng. *Acc. Chem. Res.*, **44**, 1105 (2011)
130. M.R.Hamblin. *Trends Photochem. Photobiol.*, **9**, 1 (2002)
131. H.Li, D.E.Marotta, S.Kim, T.M.Busch, E.P.Wileyto, G.J.Zheng. *J. Biomed. Opt.*, **10**, 41203 (2005)
132. B.A.Allison, E.Waterfield, A.M.Richter, J.G.J.Levy. *Photochem. Photobiol. Sci.*, **54**, 709 (1991)
133. P.C.De Smidt, A.J.Versluis, T.J.C.Van Berkel. *Biochemistry*, **32**, 2916 (1993)
134. D.Kessel, P.Thompson, S.Saatio, K.D.Nantwi. *Photochem. Photobiol.*, **45**, 787 (1987)
135. W.Cao, K.K.Ng, I.Corbin, Z.Zhang, L.Ding, J.Chen, G.Zheng. *Bioconjug. Chem.*, **20**, 2023 (2009)
136. D.E.Marotta, W.Cao, E.P.Wileyto, H.Li, I.Corbin, E.Rickter, J.D.Glickson, B.Chance, G.Zheng, T.M.Busch. *Nanomedicine*, **6**, 475 (2011)
137. L.Cui, Q.Lin, C.S.Jin, W.Jiang, H.Huang, L.Ding, N.Muhanna, J.C.Irish, F.Wang, J.Chen, G.Zheng. *ACS Nano*, **9**, 4484 (2015)
138. J.Nicolas, S.Mura, D.Brambilla, N.Mackiewicz, P.Couvreur. *Chem. Soc. Rev.*, **42**, 1147 (2013)
139. M.R.Saboktakin, R.M.Tabatabae. *Int. J. Biol. Macromol.*, **65**, 398 (2014)
140. H.De Oliveira, J.Thevenot, S.Lecommandoux. *WIREs Nanomed. Nanobiotechnol.*, **4**, 525 (2012)
141. M.Elsabahy, G.S.Heo, S.-M.Lim, G.Sun, K.L.Wooley. *Chem. Rev.*, **115**, 10967 (2015)
142. Y.-E.K.Lee, R.Kopelman, in *Biomedical Nanotechnology: Methods and Protocols*. (*Ser. Methods in Molecular Biology*. Vol. 726). (Ed. S.J.Hurst). (Totowa, NJ: Humana Press, 2011). P. 151
143. E.S.Severin. *Russ. Chem. Rev.*, **84**, 43 (2015)
144. M.Overchuk, G.Zheng. *Biomaterials*, **156**, 217 (2018)
145. D.Schmaljohann. *Adv. Drug Deliv. Rev.*, **58**, 1655 (2006)
146. F.Meng, Z.Zhong, J.Feijen. *Biomacromolecules*, **10**, 197 (2009)
147. K.Huh, H.Kang, Y.Lee, Y.Bae. *Macromol. Res.*, **20**, 224 (2012)
148. J.M.Lu, X.Wang, C.Marin-Muller, H.Wang, P.H.Lin, Q.Yao, C.Chen. *Expert Rev. Mol. Diagn.*, **9**, 325 (2009)
149. R.Gref, M.Lück, P.Quellec, M.Marchand, E.Dellacherie, S.Harnisch, T.Blunk, R.Müller. *Colloids Surf., B*, **18**, 301 (2000)
150. K.-i.Ogawara, T.Shiraishi, T.Araki, T.-i.Watanabe, T.Ono, K.Higaki. *Eur. J. Pharm. Sci.*, **82**, 154 (2016)

151. R.Z.Xiao, Z.W.Zeng, G.L.Zhou, J.J.Wang, F.Z.Li, A.M.Wang. *Int. J. Nanomed.*, **5**, 1057 (2010)
152. E.M.Cohen, H.Ding, C.W.Kessinger, C.Khemtong, J.Gao, B.D.Sumer. *Otolaryngol. Head Neck Surg.*, **145**, 612 (2011)
153. S.Pramual, K.Lirdprapamongkol, J.Svasti, M.Bergkvist, V.Jouan-Hureaux, P.Arnoux, C.Frochot, M.Barberi-Heyob, N.Niamsiri. *J. Photochem. Photobiol., B*, **173**, 12 (2017)
154. A.Vargas, M.Eid, M.Fanchaouy, R.Gurny, F.Delie. *Eur. J. Pharm. Biopharm.*, **69**, 43 (2008)
155. J.Grünebaum, J.Söbbing, D.Mulac, K.Langer. *Int. J. Pharm.*, **496**, 942 (2015)
156. H.Park, K.Na. *Biomaterials*, **34**, 6992 (2013)
157. K.Chang, Y.Tang, X.Fang, S.Yin, H.Xu, C.Wu. *Biomacromolecules*, **17**, 2128 (2016)
158. L.Li, M.Huh. *Biomater. Res.*, **18**, 19 (2014)
159. C.L.Silva, J.O.Ciampo, F.C.Rosetti, M.V.L.B.Bentley, M.B.R.Pierre. *Photochem. Photobiol.*, **89**, 1176 (2013)
160. E.Boix-Garriga, P.Accdo, A.Casado, A.Villanueva, J.C.Stockert, M.Canete, M.Mora, M.L.Sagristá, S.Nonell. *Nanotechnology*, **26**, 365104 (2015)
161. W.Shi, Y.Yin, Y.Wang, B.Zhang, P.Tan, T.Jiang, H.Mei, J.Deng, H.Wang, T.Guo, Z.Pang, Y.Hu. *Oncotarget*, **8**, 32212 (2017)
162. X.Q.Liu, C.Picart. *Adv. Mater.*, **28**, 1295 (2016)
163. S.Maiolino, F.Moret, C.Conte, A.Fraix, P.Tirino, F.Ungaro, S.Sortino, E.Reddi, F.Quaglia. *Nanoscale*, **7**, 5643 (2015)
164. Y.N.Konan-Kouakou, R.Boch, R.Gurny, E.Allemann. *J. Control. Release*, **103**, 83 (2005)
165. R.Kerdous, F.Sureau, A.Boura, S.Bonneau. *Int. J. Pharm.*, **495**, 750 (2015)
166. E.Boix-Garriga, F.Bryden, H.Savoie, M.L.Sagristá, M.Mora, R.W.Boyle, S.Nonell. *J. Porphyrins Phthalocyanines*, **20**, 1 (2016)
167. K.Jeong, S.Park, Y.-D.Lee, C.S.Kang, H.J.Kim, H.Park, I.C.Kwon, J.Kim, C.R.Park, S.Kim. *Colloids Surf., B*, **144**, 303 (2016)
168. K.E.Park, Y.-W.Noh, A.Kim, Y.T.Lim. *Carbohydr. Polym.*, **157**, 476 (2017)
169. A.S.Lavado, V.M.Chauhan, A.A.Zen, F.Giuntini, D.R.E.Jones, R.W.Boyle, A.Beeby, W.C.Chan, J.W.Aylott. *Nanoscale*, **7**, 14525 (2015)
170. S.Y.Park, H.J.Baik, Y.T.Oh, K.T.Oh, Y.S.Youn, E.S.Lee. *Angew. Chem., Int. Ed.*, **50**, 1644 (2011)
171. N.M.Oh, D.S.Kwag, K.T.Oh, Y.S.Youn, E.S.Lee. *Biomaterials*, **33**, 1884 (2012)
172. X.-H.Dai, H.Jin, M.-H.Cai, H.Wang, Z.-P.Zhou, J.-M.Pan, X.-H.Wang, Y.-S.Yan, D.-M.Liu, L.Sun. *React. Funct. Polym.*, **89**, 9 (2015)
173. A.Mero, M.Campisi. *Polymers*, **6**, 346 (2014)
174. S.Misra, P.Heldin, V.C.Hascall, N.K.Karamanos, S.S.Skandalis, R.R.Markwald, S.Ghatak. *FEBS J.*, **278**, 1429 (2011)
175. W.Li, C.Zheng, Z.Pan, C.Chen, D.Hu, G.Gao, S.Kang, H.Cui, P.Gong, L.Cai. *Biomaterials*, **101**, 10 (2016)
176. F.Li, B.-C.Bae, K.Na. *Bioconjug. Chem.*, **21**, 1312 (2010)
177. J.Han, W.Park, S.Park, K.Na. *ACS Appl. Mater. Interfaces*, **8**, 7739 (2016)
178. H.Sun, S.Li, W.Qi, R.Xing, Q.Zou, X.Yan. *Colloids Surf., A*, **538**, 795 (2018)
179. L.Upadhyaya, J.Singh, V.Agarwal, R.P.Tewari. *Carbohydr. Polym.*, **91**, 452 (2013)
180. J.Zhang, W.Xia, P.Liu, Q.Cheng, T.Tahirou, W.Gu, B.Li. *Mar. Drugs*, **8**, 1962 (2010)
181. J.C.Fernandes, X.Qiu, F.M.Winnik, M.Benderdour, X.Zhang, K.Dai, Q.Shi. *Int. J. Nanomed.*, **7**, 5833 (2012)
182. F.Q.Hu, X.H.Jiang, X.Huang, X.L.Wu, H.Yuan, X.H.Wei, Y.Z.Du. *J. Drug Target*, **17**, 384 (2009)
183. S.J.Lee, K.Park, Y.-K.Oh, S.-H.Kwon, S.Her, I.-S.Kim, K.Choi, S.J.Lee, H.Kim, S.G.Lee, K.Kim, I.C.Kwon. *Biomaterials*, **30**, 2929 (2009)
184. S.J.Lee, H.Koo, D.-E.Lee, S.Min, S.Lee, X.Chen, Y.Choi, J.F.Leary, K.Park, S.Y.Jeong, I.C.Kwon, K.Kim, K.Choi. *Biomaterials*, **32**, 4021 (2011)
185. H.M.Lee, Y.-I.Jeong, D.H.Kim, T.W.Kwak, C.-W.Chung, C.H.Kim, D.H.Kang. *Int. J. Pharm.*, **454**, 74 (2013)
186. I.-h.Oh, H.S.Min, L.Li, T.H.Tran, Y.Lee, I.C.Kwon, K.Choi, K.Kim, K.M.Huh. *Biomaterials*, **34**, 6454 (2013)
187. J.Wu, S.Feng, W.Liu, F.Gao, Y.Chen. *Int. J. Pharm.*, **528**, 287 (2017)
188. Ya.A.Ivanenkov, S.Yu.Maklakova, E.K.Beloglazkina, N.V.Zyk, A.G.Nazarenko, A.G.Tonevitsky, V.E.Kotelianski, A.G.Majouga. *Russ. Chem. Rev.*, **86**, 750 (2017)